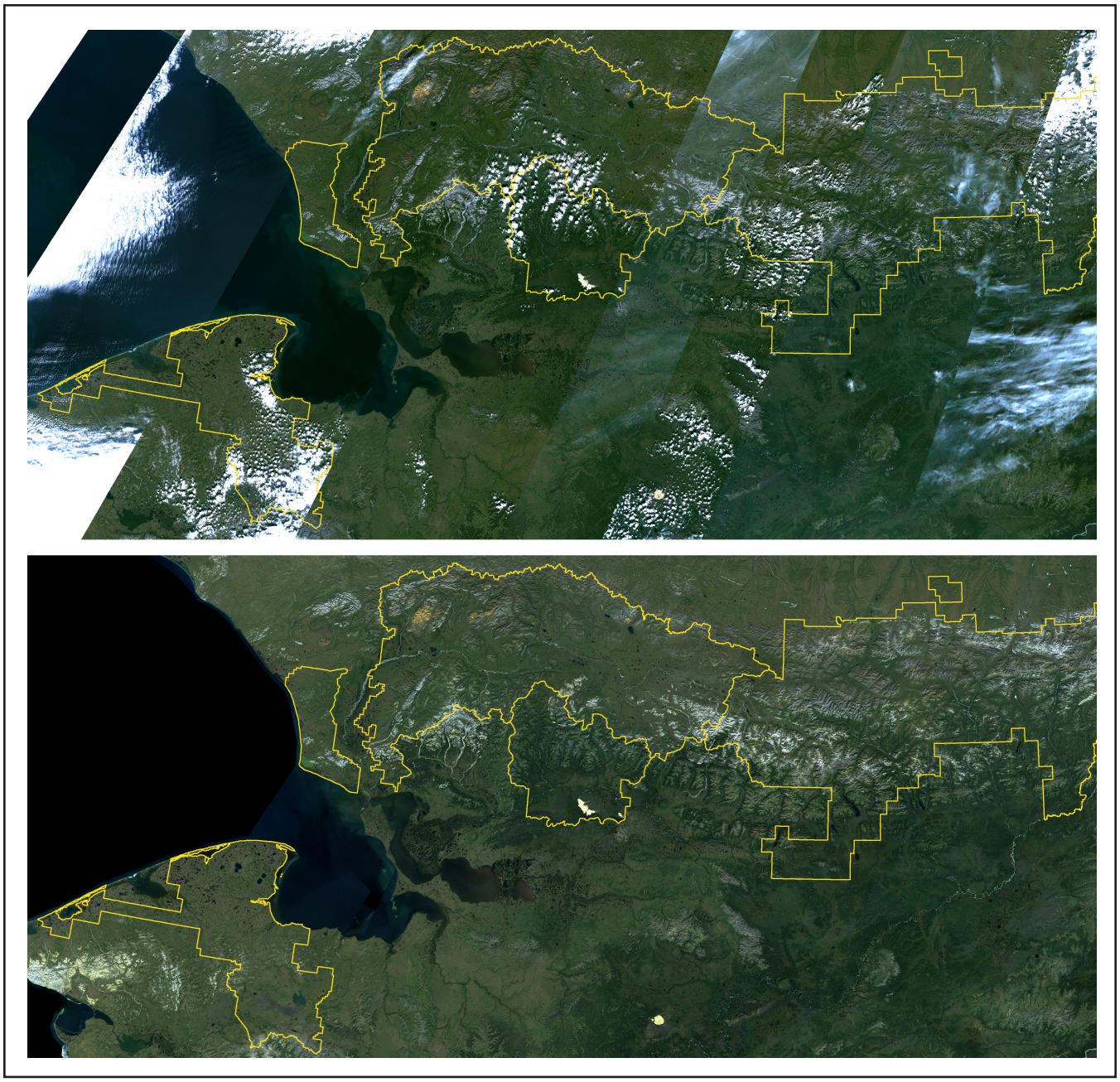
National Park Service
U.S. Department of the Interior

Natural Resource Program Center

A Surface Reflectance Calibrated Landsat Mosaic (circa 2002) for the Arctic Network of National Parks

Natural Resource Technical Report NPS/ARCN/NRTR—2010/393



ON THE COVER

Arctic Network of National Parks and surrounding areas, Alaska.

Top: Eight Landsat ETM+ swaths, acquired 24 July through 4 August 2002. WRS2 Paths 72–83, Rows 11–15. Calibrated to top-of-atmosphere reflectance.

Bottom: Cloud-free Landsat mosaic, circa 1 August 2002. Calibrated to surface reflectance.

Maps courtesy ABR, Inc.

A Surface Reflectance Calibrated Landsat Mosaic (circa 2002) for the Arctic Network of National Parks

Natural Resource Technical Report NPS/ARCN/NRTR—2010/393
Matthew J. Macander
ABR, Inc.—Environmental Research & Services
P.O. Box 80410
Fairbanks, AK 99708

December 2010

U.S. Department of the Interior
National Park Service
Natural Resource Program Center
Fort Collins, Colorado

The National Park Service, Natural Resource Program Center publishes a range of reports that address natural resource topics of interest and applicability to a broad audience in the National Park Service and others in natural resource management, including scientists, conservation and environmental constituencies, and the public.

The Natural Resource Technical Report Series is used to disseminate results of scientific studies in the physical, biological, and social sciences for both the advancement of science and the achievement of the National Park Service mission. The series provides contributors with a forum for displaying comprehensive data that are often deleted from journals because of page limitations.

All manuscripts in the series receive the appropriate level of peer review to ensure that the information is scientifically credible, technically accurate, appropriately written for the intended audience, and designed and published in a professional manner.

This report received informal peer review by subject-matter experts who were not directly involved in the collection, analysis, or reporting of the data.

Views, statements, findings, conclusions, recommendations, and data in this report do not necessarily reflect views and policies of the National Park Service, U.S. Department of the Interior. Mention of trade names or commercial products does not constitute endorsement or recommendation for use by the U.S. Government.

This report is available from http:/science.nature.nps.gov/im/units/arcn and the Natural Resource Publications Management Web site (http://www.nature.nps.gov/publications/NRPM) on the Internet.

Please cite this publication as:

Macander, M. J. 2010. A surface reflectance calibrated Landsat mosaic (circa 2002) for the Arctic Network of National Parks. Natural Resource Technical Report NPS/ARCN/NRTR—2010/393. National Park Service, Fort Collins, Colorado.

NPS 953/105935, December 2010

Contents

Figures iv
Tables iv
Appendices iv
Acknowledgments v
Introduction 1
Study Area 1
Methods 2
Snap Raster 2
Image Acquisition and Preprocessing 2
Radiometric Normalization 4
Image-to-Image Radiometric Calibration 4
Surface Reflectance 4
Radiometric Normalization Evaluation 5
Mosaicking 5
Digital Elevation Model Preprocessing 6
Topographic Normalization 6
Results 9
Image Acquisition and Preprocessing 9
Radiometric Normalization 9
Image-to-Image Radiometric Calibration 9
Surface Reflectance 10
Radiometric Normalization Evaluation 15
Mosaicking 19
DEM Preprocessing 20
Topographic Normalization 20
Conclusions 24
Literature Cited 33

Figures

Figure 1. Primary and Full Study Area for Arctic Park Network Landsat Mosaic 1
Figure 2. Coverage of Landsat WRS2 Paths over ARCN Landsat Mosaic Full Study Area. 10
Figure 3. Visual comparison of calibrated top-of-atmosphere reflectance and surface reflectance for selected Landsat swaths. 13
Figure 4. Visual comparison of Landsat top-of-atmosphere reflectance, Landsat surface reflectance, and eMODIS surface reflectance 16
Figure 5. Reflectance difference in overlapping portion of Landsat swaths with two radiometric normalization approaches 17
Figure 6. Reflectance difference in overlapping portion of Landsat swaths with two radiometric normalization approaches. 18
Figure 7. Arctic Park Network Landsat mosaic, circa 2002 21
Figure 8. Arctic Park Network Landsat mosaic metadata and derived products 22
Figure 9. Visual comparison of hillshades from ASTER G-DEM and NED DEM 23
Figure 10. Topographically normalized Landsat mosaic, circa 2002 31

Tables

Table 1. Contrast stretch parameters for display on top-of-atmosphere and surface reflectance images 3
Table 2. Landsat TM and ETM+ bands and corresponding MODIS bands 5
Table 3. Slope bins used to stratify topographic normalization sample data 7
Table 4. Aspect bins used to stratify topographic normalization sample data 8
Table 5. NDVI bins used to stratify topographic normalization sample data 8
Table 6. Range of WRS2 rows for each path in study area 9
Table 7. Landsat swaths considered for the mosaic 11
Table 8. Calibration coefficients for image-to-image radiometric calibration using Landsat 7 ETM+ swath acquired 29 July 2002, WRS2 path 78 as reference image 12
Table 9. Landsat TM/ETM+ band 1 Minnaert k values as a function of slope and NDVI 25
Table 10. Landsat TM/ETM+ band 2 Minnaert k values as a function of slope and NDVI 26
Table 11. Landsat TM/ETM+ band 3 Minnaert k values as a function of slope and NDVI 27
Table 12. Landsat TM/ETM+ band 4 Minnaert k values as a function of slope and NDVI 28
Table 13. Landsat TM/ETM+ band 5 Minnaert k values as a function of slope and NDVI 29
Table 14. Landsat TM/ETM+ band 7 Minnaert k values as a function of slope and NDVI 30

Appendices

Appendix 1. Data deliverable overview 34
Appendix 2. List and description of scripts used to generate the Landsat mosaic products 36
Appendix 3. Landsat scenes considered formosaic with selected metadata values 39

Acknowledgments

We thank Jim Lawler and Parker Martyn with the National Park Service for support and management of this project. Scott Miller with the National Park Service provided advice on metadata documentation for the data deliverable. Chris Swingley was instrumental in developing many of the image processing scripts. Aaron Wells, Allison Zusi-Cobb, Beth Koltun, Dave Swanson, and Dave Verbyla provided helpful review comments. We give Pam Odom a special thanks for producing this report.

Introduction

The Arctic Network (ARCN) of the National Park Service's (NPS) Inventory and Monitoring Program (I&M) is developing a long-term monitoring program to assess ecological changes in five parks in northwestern Alaska: Bering Land Bridge National Preserve (BELA), Cape Krusenstern National Monument (CAKR), Noatak National Preserve (NOAT), Kobuk Valley National Park (KOVA) and Gates of the Arctic National Park and Preserve (GAAR). As part of this effort, a Landsat mosaic that includes all of the Arctic Network park units was prepared. Most of the mosaic was covered by Landsat imagery acquired during a three week period in late July and early August 2002. Radiometric normalization was performed to minimize atmospheric effects, resulting in a mosaic with consistent and physically based properties. Two calibration approaches were evaluated (1) calibration to a target Landsat image and (2) calibration to a surface reflectance. The final mosaic was calibrated to surface reflectance, which improves the ability to perform spectral analyses over the full extent of the mosaic, and provides a robust basis for change detection and other time series studies. In addition, a topographic normalization procedure was performed on the mosaic to reduce the topographic effects of sun and terrain angles on the imagery. The deliverables include the mosaic products in digital format, coefficients and GIS layers necessary to produce the mosaic, and scripts used to automate the process.

Study Area

The boundaries of the five ARCN NPS units and Selawik National Wildlife Refuge (SWK) were buffered by 12 miles. Selected areas that were mostly surrounded by the unit buffers were added, and this polygon defined the primary study area (Figure 1). The horizontal coordinate system was

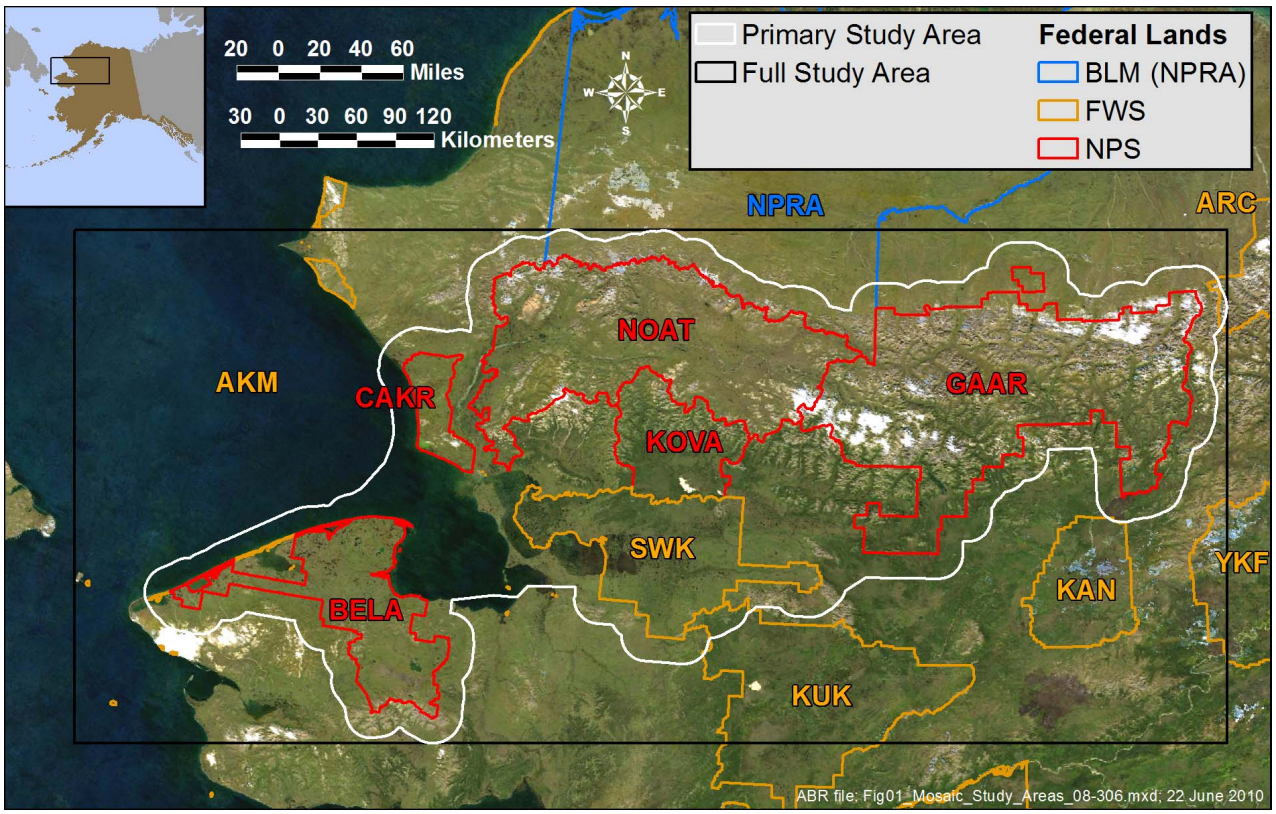


Figure 1. Primary and full study area for Arctic Park Network (ARCN) Landsat Mosaic.

established as Alaska Albers (NAD 1983). The rectangular bounding box for the primary study area was expanded to the west to cover Cape Wales and the Diomede Islands. The expanded bounding box defined the total area covered by the mosaic, and is referred to as the full study area (Figure 1).

Though image acquisition was focused on the areas within the primary study area, the coverage of Landsat swaths allowed adjacent areas to be covered with minimal additional effort. These additional areas included southern National Petroleum Reserve—Alaska (NPRA), Kanuti National Wildlife Refuge (KAN) and portions of Koyukuk (KUK), Yukon Flats (YKF), Arctic (ARC), and Alaska Maritime (AKM) National Wildlife Refuges. The full study area ranged from 149.0–169.1 west longitude, an east–west distance of 894 km; and from 64.8–68.9 north latitude, a north–south distance of 399 km. Excluding offshore ocean areas from the full study area, the total surface area covered was 290,164 square kilometers.

Methods

Snap Raster

The study area was converted to a raster at 30-m resolution in the Alaska Albers (NAD 1983) coordinate system. The cell alignment of the 30-m pixels was set so that all of the products from this effort would align exactly with the Web-Enabled Landsat Data (WELD, Roy 2010a) product for Alaska. WELD data will likely be a primary source of new Landsat data in the near future. The WELD data is aligned on a snap grid such that one of the WELD pixels has the Alaska Albers (NAD 1983) coordinate (0,10) located at the center of the pixel, with all other pixels aligned in 30-m offsets. The snap raster is important because without a consistent cell alignment, pixel locations may shift up to 15-m in both the X and Y directions when data from different images are mosaicked, or when calculations are performed using multiple images.

Image Acquisition and Preprocessing

The World Reference System 2 (WRS2) system is used to organize imagery from the Landsat 3, 4, 5 and 7 satellites into paths and rows. All the ascending (daytime) WRS2 Landsat paths and rows that intersect the full study area were identified, and the corresponding browse images were downloaded from the USGS. Landsat browse images are Joint Photographic Experts Group (JPEG) format image files with ~250-m resolution. Each browse image has an associated text file with metadata information. The browse images were organized into folders by WRS2 path/rows. The metadata for each browse image was used to construct an ArcGIS-compatible world file (used to provide georeferencing information for the browse image). The browse images were renamed by prepending the text "MM-DD-YYYY_" to the filename of each browse image and world file (MM is the two digit month, DD is the two digit day of month, and YYYY is the four digit year). The prepended text enabled the browse images to be sorted by day of year, which allowed a quick visual review of all the available browse images from a specific time of year. In areas where the late July and early August 2002 imagery provided complete cloud-free coverage (primarily the western third of the study area), no additional imagery was identified. In other areas, where cloud cover was known to contaminate portions of the late July and early August 2002 imagery, all scenes between late June and early September with clear atmospheric conditions and minimal cloud cover were identified.

The scenes were submitted to the USGS Landsat bulk download page (http://edcsns17.cr.usgs.gov/EarthExplorer/order/bulkDownload.php). This web page provides links to scenes that are

available for download as well as an interface to the ordering system for scenes that are not available but that can be processed for free upon request. After the scene processing was completed, the data were obtained using a set of scripts that downloaded and unpacked the data, read the associated metadata file and wrote the results to a PostgreSQL database table.

The metadata tables were reviewed to identify the processing level for each scene. Terrain Corrected (L1T) scenes have very precise geolocation based on the inclusion of ground control points from Landsat GeoCover images. These scenes are accurately coregistered to each other (generally within one 30-m pixel). Systematic Corrected (L1G) scenes lack ground control points and have lower geolocation precision. Several of the scenes initially obtained in 2008 were processed to L1G initially and were not coregistered well to the other data. However, these scenes were re-ordered in 2009 or 2010 and the newer processing system successfully processed them to L1T. Only L1T scenes were used for this effort.

Scenes were converted to top-of-atmosphere reflectance using the scene metadata and calibration coefficients from the Landsat 7 Science Data Users Handbook (http://landsathandbook.gsfc.nasa.gov/handbook.html). Landsat 4 and 5 data were calibrated using the coefficients from Chander et al. 2009. The gain and bias values required to convert each band to radiance and reflectance were calculated and stored in the metadata table for each scene.

Full resolution, six band, contrast calibrated browse images in JPEG 2000 format were generated for each downloaded image. The contrast calibration was based on fixed top-of-atmosphere reflectance values that were selected to optimize the contrast in cloud-free areas of typical summer scenes in Northwest Alaska (Table 1). The contrast stretches are written to the .aux.xml header file associated with each JPEG 2000 image, stored as the statistics for each band. While actual image statistics result in image contrast stretches that are sensitive to the extent of snow, ice, water and clouds in each image, fixed reflectance values provide a consistent appearance across different images. The fixed reflectance values are converted to the 8-bit digital number (DN) values of the raw imagery and are stored as the minimum, maximum, mean and standard deviation values for each band. These statistics populate the default two-standard deviation contrast stretch parameters when displayed in

Table 1. Contrast stretch parameters for display of top of atmosphere and surface reflectance images.

Landsat TM/ETM+ Band	Top of Atmosphere Reflectance		Surface Reflectance	
	Min	Max	Min	Max
1	0.080	0.200	0.000	0.180
2	0.035	0.220	0.000	0.200
3	0.030	0.250	0.000	0.250
4	0.000	0.500	0.000	0.500
5	0.000	0.350	0.000	0.350
7	0.000	0.200	0.000	0.200

ArcCatalog, ArcMap or other image viewing applications.

Following review of the full resolution browse images, 40 Landsat swaths were selected for consideration in the mosaicking process. A 16-bit signed-integer format GeoTiff was generated for each scene in the selected swaths. Reflectance values were scaled by a factor of 10,000. The calibrated scenes were reprojected from the source UTM projection (WGS 1984 horizontal datum) to Alaska Albers (NAD1983 horizonatal datum) using nearest neighbor resampling, the NAD_1983_TO_WGS_1984_5 datum transformation, 30-m cell size, and the standard snap raster. Adjacent scenes from the same acquisition date were then mosaicked into swaths that were clipped to the full study area bounds. Fixed contrast stretches for each swath were encoded as band statistics in the .aux.xml header file (Table 1, top of atmosphere reflectance). 8-bit versions of each swath were also generated for faster display performance using the same contrast stretch parameters.

Radiometric Normalization

Radiometric normalization standardizes Landsat data that were acquired on different dates, under different atmospheric conditions and solar geometry, and in some cases using different sensors. Two approaches to radiometric normalization were assessed: calibration to a target Landsat image (image-to-image calibration) and calibration to surface reflectance.

Image-to-Image Radiometric Calibration

For the image-to-image calibration, the primary reference imagery was the Landsat ETM+ swath acquired July 29, 2002 (path 78, rows 11–15). The objective of image-to-image calibration is to correct the other scenes so that their pixel values were compatible with those of the primary image. Corrections were needed mainly to account for the effects of different atmospheric conditions on different acquisition dates. Scenes that did not overlap the primary swath were normalized using Landsat images that had already been normalized.

We developed a preliminary cloud mask for each scene. We generated a set of stratified random points for the mosaic area, to ensure that the full range of scene brightness was represented, including rarer, bright pixels. Points within the preliminary cloud mask were excluded. Random points were used to sample the reference image and the target images, and the resulting values were assessed interactively using scatterplots in ArcMap. The sample set was screened to filter out snow, small clouds, and calibration points located near abrupt brightness changes. A table containing the resulting set of filtered points was analyzed in a statistical package to determine linear regression coefficients. The normalization then applied these coefficients to the target image.

Surface Reflectance

Surface reflectance was calculated for each scene using the Landsat Ecosystem Disturbance Adaptive Processing System (LEDAPS, http://ledaps.nascom.nasa.gov/, Masek 2006). LEDAPS subroutines calculate top of atmosphere reflectance, a cloud mask, aerosol optical depth and surface reflectance for each scene. Surface reflectance is calculated using the Second Simulation of the Satellite Signal in the Solar Spectrum (6S) vector code (Kotchenova 2006) with ancillary inputs of tropospheric ozone, column water vapor and aerosol optical thickness (AOT). Daily maps of the ozone and water vapor data were provided with the code, while the AOT was estimated from the imagery using the dark, dense vegetation (DDV) method (Kaufman 1997, Remer 2005).

LEDAPS produced an eight-band surface reflectance output in HDF format for each scene. The first six bands were Landsat bands 1–5 and 7; the seventh band was the AOT, and the eighth contained QA/QC values. The HDF file

was converted to GeoTiff and was reprojected from the source UTM projection (WGS 1984 horizontal datum) to Alaska Albers (NAD1983 horizonatal datum) using nearest neighbor resampling, the NAD_1983_TO_WGS_1984_5 datum transformation, 30-m cell size, and the standard snap raster. The solar zenith and solar azimuth angle for each scene were extracted from the metadata table and were written as bands that were appended to the first seven bands in the reprojected LEDAPS image. Adjacent scenes from the same acquisition date were then mosaicked into swaths that were clipped to the full study area bounds. Fixed contrast stretches for each swath were encoded as band statistics in the .aux.xml header file (Table 1, surface reflectance), and 8-bit versions were generated for faster display performance.

Radiometric Normalization Evaluation

The results of the two radiometric calibration approaches were assessed visually, by comparing the same swath calibrated by the two approaches. Selected swaths were visually compared to the eMODIS 500m composite data (Jenkerson and Schmidt 2009) from the same date range. eMODIS products are a 7-day dataset over Alaska based on surface reflectance calibrated data from the Moderate Resolution Imaging Spectroradiometer (MODIS) sensor on the Terra satellite. Landsat and MODIS bands were matched for comparison based on Table 2. In addition to visual comparisons, image differencing was used to calculate the difference in reflectance values in the overlap area between pairs of Landsat swaths with very close acquisition dates, where real change in reflectance would be unlikely.

Mosaicking

A set of mosaic map layers (non-overlapping vector polygon datasets) was maintained that identified which scene would be passed through to the final mosaic for each region of the study area. Mosaic maps were maintained for three eras: 2002 scenes, 1999 scenes, and the "alternate" scenes which included data from other years to fill in small patches that were cloud-covered in both 1999 and 2002. The construction of the final mosaic map for each era was an iterative process in which a mosaic was created and reviewed visually, adjustments were made to the mosaic map layer, the mosaic was regenerated, and the process was repeated. A final mosaic map was then constructed that identified the source era for each pixel in the final mosaic. When completed, the mosaic was maintained at 16-bit radiometric resolution (reflectance scaled by 10,000). In addition, we produced an 8-bit version

Table 2. Landsat TM and ETM+ bands and corresponding MODIS bands.

Landsat Band	Wavelength Interval	Spectral Response	Corresponding MODIS Band
1	0.45-0.52 µm	Blue-Green	3
2	0.52-0.60 µm	Green	4
3	0.63-0.69 µm	Red	1
4	0.76-0.90 µm	Near IR	2
5	1.55-1.75 µm	Mid-IR	6
6	10.40-12.50 µm	Thermal IR	
7	2.08-2.35 µm	Mid-IR	7

using the scales and offsets defined in Table 1 (surface reflectance). The mosaic map layer allowed the scene specific information (such as date, solar elevation and azimuth) to be compiled for all portions of the mosaic.

Digital Elevation Model (DEM) Preprocessing

DEM data are required inputs for the illumination normalization procedure described below. Two sources of DEM data were considered: the National Elevation Dataset (NED) and the Advanced Spaceborne Thermal Emission and Reflection Radiometer (ASTER) Global Digital Elevation Model (G-DEM), a product of the Ministry of Economy, Trade and Industy (METI) and the National Aeronautical and Space Administration (NASA). The ASTER G-DEM has higher resolution and is based on data that is much more recent than the NED.

The raw data for NED (2 arc-second, approximately 26-m east-west by 60-m north-south resolution) and G-DEM (1 arc-second, approximately 13-m east-west by 30-m north-south resolution) were obtained. Each DEM was reprojected to Alaska Albers (NAD 1983) using bilinear resampling, 30-m cell size, and the standard snap raster. The NED DEM was then shifted 60 m north, based on a geolocation evaluation performed for the ARCN ecotype mapping project (Jorgenson 2009).

There is a distortion of direction in the Alaska Albers coordinate system which is most pronounced near the corners of the state, such as the study area. The direction distortion would bias calculations that depend on the topographic aspect—in particular, the solar incidence angle.

To quantify direction distortion and correct for it, a decimal degree grid covering the study area at 0.1 degree resolution was created, with the value of each cell set equal to longitude. Because the longitude increases monotonically from left to right, the aspect for each cell in the grid was equal to 270 (west-facing). The longitude grid was then reprojected into Alaska Albers and the aspect was recalculated. The grid was still generally west-facing but was not precisely equal to 270 degrees. The difference between 270 and the aspect of the reprojected grid was the direction distortion. The adjusted aspect was calculated as the DEM-derived aspect plus the direction distortion; 360 was subtracted from adjusted aspect values greater than 360.

The two DEMs were compared to assess their suitability for the topographic normalization routine. The elevation difference between the two DEMs was computed, and a visual comparison was performed, primarily using the DEM derivative hillshade.

Topographic Normalization

The radiometric calibration and normalization techniques described above do not address the problem of topographic effects on remote-sensing imagery. ARCN contains extensive areas of hilly and mountainous terrain, where these topographic effects are most pronounced. Sun angles are low at high latitudes, which further increases topographic effects. To minimize these effects, we performed an illumination normalization procedure and a backwards radiance correction transformation (Colby 1991). The Minnaert correction model is expressed as:

(Equation 1) $\rho_H = \rho_T * \cos e / (\cos e \cos i)^k$

where ρ_H is the equivalent reflectance on a flat surface with incident angle of zero, ρ_T is the observed reflectance, e is the terrain slope, i is the solar incidence angle (the angle between the terrain normal and the solar radiation), and k is the Minnaert value. The cosine of the solar incidence angle ($\cos i$) is calculated as:

(Equation 2) $\cos i = \cos \theta \cos e + \sin \theta \sin e \cos(\varphi_m - \varphi_s)$

where θ = solar zenith angle, φ_s = solar azimuth, e = terrain slope, and φ_m = terrain aspect.

Reformulating equation 1 results in:

(Equation 3) $\ln(\rho_T \cos e) = \ln \rho_T + k \ln(\cos e \cos i)$

Equation 3 indicates that k is the slope of the regression line when $\ln(\rho_T \cos e)$ is the dependent variable and $\ln(\cos e \cos i)$ is the independent variable. Therefore k can be estimated from regression analysis when the slope, solar incidence angle, and reflectance are known. The k value is sometimes referred to as a constant but it varies for each band, and is also known to vary with different land cover types and different slopes (Lu 2008). Lu related the k value to slope, while we related the k value to both slope and the Normalized Difference Vegetation Index (NDVI). NDVI is fairly resistant to topographic effects and was used to distinguish a gradient of barren, partially vegetated, and densely vegetated land cover types for the illumination normalization. We modeled k as a function of band, slope, and NDVI and then calculated k-images for each band.

The NED DEM data were selected for use in the topographic normalization procedure. To perform the illumination correction, the NED DEM data were compiled and several derivatives were calculated. These included the slope, aspect, and solar incidence angle. We used the adjusted aspect (corrected for the map projection distortion; see above) for this analysis. The mosaic area was stratified into categories based on slope (Table 3), aspect (Table 4), and NDVI (Table 5). These three stratification grids were then combined and approximately 1000 random cells were extracted for each unique combination of slope, aspect and NDVI category. This ensured that a full range of illumination conditions and vegetation index values were sampled.

The set of points were used to sample the mosaic pixel values, DEM derivatives, and NDVI. We analyzed the variability of the estimated k-value in relation to band, slope, and NDVI; and produced models to calculate k-images for each band as a function of NDVI and slope. The k-images were used to define the correction factor for each band:

(Equation 4) $F_b = \cos e / (\cos e \cos i)^k$,

where F_b is the correction factor, which is applied to produce the topographically normalized image:

(Equation 5) $\rho_H = \rho_T * F_b$

Equations 4 and 5 are adapted from Equation 1. The correction factor image is a useful diagnostic to understand the magnitude of the illumination correction performed for each pixel. The topographically normalized image was stored in 16-bit signed integer format (scaled by 10,000) and was also converted to 8-bit format for display performance using the surface reflectance contrast stretch parameters (Table 1).

.

Table 3. Slope bins used to stratify topographic normalization sample data. Units are degrees of slope.

Slope Bin	Min	Max
0	0.000	0.500
2	0.501	4.500
7	4.501	9.500
12	9.501	14.500
17	14.501	19.500
22	19.501	24.500
27	24.501	29.500
32	29.501	34.500
37	34.501	39.500
45	39.501	49.500
55	49.501	80.000

Table 4. Aspect bins used to stratify topographic normalization sample data. Aspect units are degrees, and are adjusted for projection distortion.

Aspect Bin	Min	Max	Label
0	-1	-1	Flat
1	0.000	22.500	North
2	22.501	67.500	Northeast
3	67.501	112.500	East
4	112.501	157.500	Southeast
5	157.501	202.500	South
6	202.501	247.500	Southwest
7	247.501	292.500	West
8	292.501	337.500	Northwest
1	337.501	360.000	North

Table 5. NDVI bins used to stratify topographic normalization sample data. NDVI values are scaled by 10,000.

NDVI Bin	Min	Max
0	-4000	500
1	501	1500
2	1501	2500
3	2501	3500
4	3501	4500
5	4501	5500
6	5501	6500
7	6501	7500
8	7501	8500
9	8501	9500
10	9501	10000

Results

Image Acquisition and Preprocessing

Landsat WRS2 paths 70–87 crossed the study area, with between one and five rows included on each path (Table 6). The converging polar orbits of the Landsat satellites result in increasing overlap between adjacent paths approaching the poles. Within the full study area, there is usually coverage from three WRS2 paths, though there are wedges in the northern portion of the study area with coverage from four WRS2 paths, and wedges in the southern portion of the study area with coverage from two WRS2 paths (Figure 2).

A total of 958 Landsat scenes were ordered and processed to full resolution browse. Not all of the scenes were intended for consideration as part of this mosaic. Some were selected to help distinguish tall vegetation that overtopped the snowpack in early spring. Others depicted different stages of snowmelt, actively burning fires, or other features of interest. All of these scenes are included with the data deliverables and may be used for visualization or analysis. 40 swaths—each comprising 1 to 5 scenes—were selected for potential inclusion in the mosaic (Table 7).

Radiometric Normalization

Image-to-Image Radiometric Calibration

The image-to-image calibration used the Landsat swath acquired 29 July 2002 (WRS2 path 78) as the calibration target. The calibration used an earlier version of the swaths which had a different cell size (28.5-m) and in some cases different geolocation information. As a result, the original sample points cannot reliably be directly compared to the final mosaic, because many of the original sample points overlay different pixels.

Table 6. Range of WRS2 rows for each path in study area.

WRS2 Path	WRS2 Row 11	WRS2 Row 12	WRS2 Row 13	WRS2 Row 14	WRS2 Row 15
70			X	X	
71		X	X	X	
72		X	X	X	
73	X	X	X	X	
74	X	X	X	X	
75	X	X	X	X	
76	X	X	X	X	
77	X	X	X	X	X
78	X	X	X	X	X
79	X	X	X	X	X
80	X	X	X	X	X
81	X	X	X	X	X
82	X	X	X	X	X
83	X	X	X	X	X
84	X	X	X	X	
85		X	X		
86		X	X		
87		X			

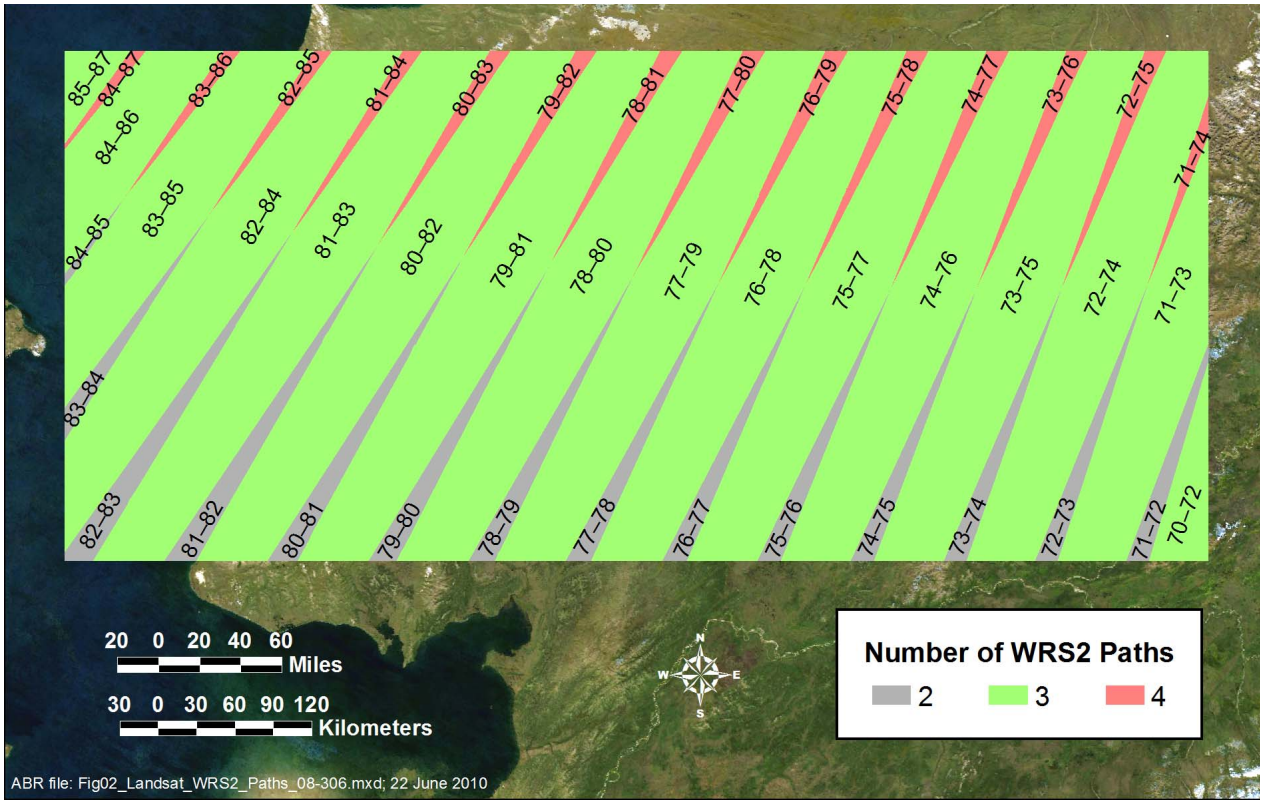


Figure 2. Coverage of Landsat WRS2 Paths over ARCN Landsat Mosaic Full Study Area.

The image-to-image calibration was performed for 9 swaths (not including the target swath). 5 of the swaths, in paths 76–80, were calibrated using only the overlap between the subject image and the calibration target. The path 75 and 81 swaths had very limited overlap with path 78 (Figure 2), and so were primarily calibrated using already calibrated images. Finally, the path 74 and path 83 swaths had no overlap with the path 78, and were entirely calibrated using other calibrated images.

The slope and offset values for the calibration of the selected swaths are presented in Table 8. For the swaths calibrated using only the path 78 calibration target (path 76, 77, 79 and 80), the offset values are increasingly negative for the swaths east of the calibration target (i.e., path 76 offsets are more negative than path 77) and increasingly positive for the swaths west of the calibration target (i.e., path 80 offsets are more positive than path 79 offsets). This suggests that there may be a systematic factor other than variable atmosphere affecting the relative brightness of each scene from east to west.

Surface Reflectance

The 40 swaths that were selected for potential inclusion in the mosaic (Table 7) were processed to surface reflectance using the LEDAPS algorithm. Of these, 14 swaths were from a 21-day period between 18 July and 7 August 2002; 30 of the selected scenes were from summer 1999 or 2002.

The atmospheric ozone data for 2–13 August 2002 had extensive occurrence of fill values instead of actual data over the study area. The LEDAPS algorithm apparently interpreted fill values as zero atmospheric ozone. To replace the fill values with more realistic values, the mean ozone values for 2–13 August in years 2000, 2001, 2003 and 2004 were computed. The mean value for each pixel was used to replace the original ancillary

Table 7. Landsat swaths considered for the mosaic.

Swath Name	Satellite	Sensor	Date	Year	WRS2 Path
L7071_20010623	7	ETM+	6/23/2001	2001	71
L5071_19990626	5	TM	6/26/1999	1999	71
L5077_20080628	5	TM	6/28/2008	2008	77
L7077_20050628	7	ETM+	6/28/2005	2005	77
L7079_20000628	7	ETM+	6/28/2000	2000	79
L7075_19990630	7	ETM+	6/30/1999	1999	75
L7073_19990702	7	ETM+	7/2/1999	1999	73
L5072_19990703	5	TM	7/3/1999	1999	72
L5078_20070703	5	TM	7/3/2007	2007	78
L5080_20080703	5	TM	7/3/2008	2008	80
L5078_20080705	5	TM	7/5/2008	2008	78
L7073_20020710	7	ETM+	7/10/2002	2002	73
L7083_20000710	7	ETM+	7/10/2000	2000	83
L7080_20020711	7	ETM+	7/11/2002	2002	80
L5071_19990712	5	TM	7/12/1999	1999	71
L7076_20030718	7	ETM+	7/18/2003	2003	76
L7081_20020718	7	ETM+	7/18/2002	2002	81
L7072_20020719	7	ETM+	7/19/2002	2002	72
L7079_20020720	7	ETM+	7/20/2002	2002	79
L5071_19850721	5	TM	7/21/1985	1985	71
L5077_20050722	5	TM	7/22/2005	2005	77
L7075_20020724	7	ETM+	7/24/2002	2002	75
L7082_20020725	7	ETM+	7/25/2002	2002	82
L7072_19990727	7	ETM+	7/27/1999	1999	72
L7080_20020727	7	ETM+	7/27/2002	2002	80
L5079_20080728	5	TM	7/28/2008	2008	79
L7079_19990728	7	ETM+	7/28/1999	1999	79
L4074_19890729	4	TM	7/29/1989	1989	74
L7078_20020729	7	ETM+	7/29/2002	2002	78
L7076_20020731	7	ETM+	7/31/2002	2002	76
L7083_20020801	7	ETM+	8/1/2002	2002	83
L7074_20020802	7	ETM+	8/2/2002	2002	74
L7073_19990803	7	ETM+	8/3/1999	1999	73
L7081_20020803	7	ETM+	8/3/2002	2002	81
L7072_20020804	7	ETM+	8/4/2002	2002	72
L7079_20020805	7	ETM+	8/5/2002	2002	79
L7077_20020807	7	ETM+	8/7/2002	2002	77
L7080_20020812	7	ETM+	8/12/2002	2002	80
L7074_20020818	7	ETM+	8/18/2002	2002	74
L7079_20020821	7	ETM+	8/21/2002	2002	79

Table 8. Calibration coefficients for image-to-image radiometric calibration using Landsat 7 ETM+ swath acquired 29 July 2002, WRS2 path 78 as reference image.

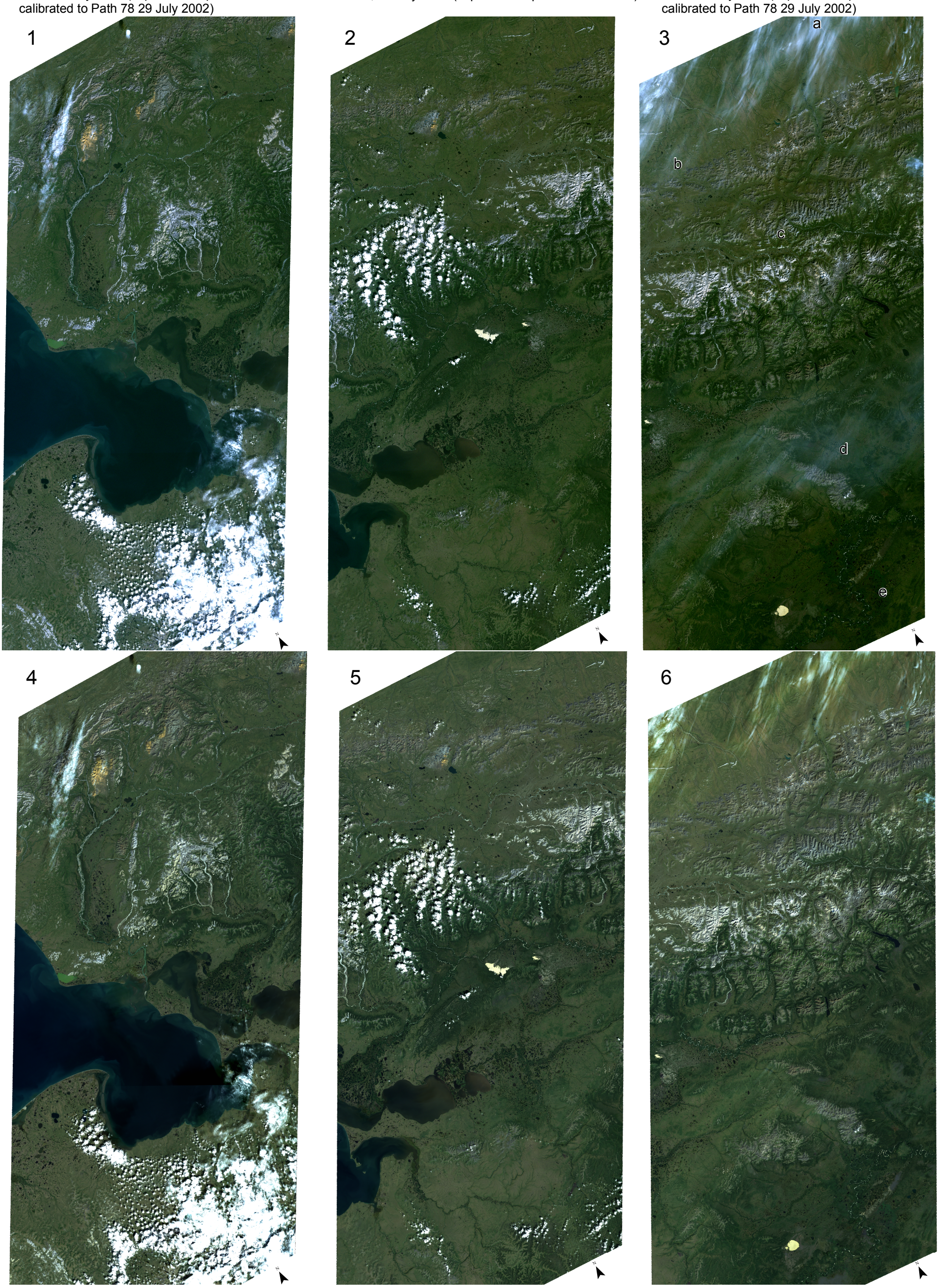
	Band 1		Band 2		Band 3		Band 4		Band 5		Band 7	
Swath	Offset	Slope	Offset	Slope	Offset	Slope	Offset	Slope	Offset	Slope	Offset	Slope
L7074_20020802[a]	-133.3	1.01598	-70.1	0.98584	-38.2	0.97576	-60.0	1.01219	28.9	0.94488	34.0	0.94998
L7075_20020724[b]	-17.0	0.98666	-23.7	0.99838	-16.9	1.00788	-15.5	0.98447	-11.7	1.00513	-1.5	1.00672
L7076_20020731	-229.2	1.09303	-164.4	1.06970	-124.0	1.05717	-211.7	1.07681	-97.9	1.03911	-48.0	1.03708
L7077_20020807	-2.2	0.97991	-16.4	0.99770	-26.5	1.00094	11.2	0.98911	20.7	0.96773	-7.8	0.98366
L7079_19990728	57.8	1.00157	32.6	1.02113	43.9	1.02175	90.4	0.93115	49.1	1.01990	40.4	1.01295
L7079_20020805	35.4	0.97135	28.5	0.95954	7.4	0.96622	214.4	0.93270	227.4	0.90097	54.4	0.93590
L7080_20020727	62.6	1.00349	43.6	1.00816	34.1	1.01002	78.1	1.00156	74.6	1.00952	37.4	1.00585
L7081_20020803[c]	-39.8	1.05287	-12.0	1.02994	14.8	1.01474	101.1	1.00569	122.0	0.99116	75.8	1.00312
L7083_20020801[d]	15.9	1.05354	34.0	1.03208	66.7	1.01763	214.3	1.00390	229.2	0.99563	146.4	1.02278

a. Calibrated to L7075_20020724 and L7076_20020731
b. Calibrated to L7076_20020731, L7077_20020807, and L7078_20020729
c. Calibrated to L7078_20020729 and L7080_20020727
d. Calibrated to L7081_20020801

Path 80, 27 July 2002 (Top-of-Atmosphere Reflectance, calibrated to Path 78 29 July 2002)

Path 78, 29 July 2002 (Top-of-Atmosphere Reflectance)

Path 76, 31 July 2002 (Top-of-Atmosphere Reflectance, calibrated to Path 78 29 July 2002)



Path 80, 27 July 2002 (LEDAPS Surface Reflectance)

Path 78, 29 July 2002 (LEDAPS Surface Reflectance)

Path 76, 31 July 2002 (LEDAPS Surface Reflectance)

Figure 3: Visual Comparison of Calibrated Top-of-Atmosphere Reflectance and Surface Reflectance for Selected Landsat Swaths.

20 0 20 40 Miles

20 0 20 40 60 Kilometers

ABR file: Fig03_RadCal_vs_LEDAPS_Visual321.mxd; 10 June 2010

ozone data for the corrupted time period. While this map of typical ozone levels for early August 2002 was not as accurate as the actual daily observations of ozone, these data should provide more realistic results as compared to using the corrupted data which were interpreted as zero ozone.

Radiometric Normalization Evaluation

The image-to-image calibration produces a single correction for each swath, and therefore does not handle within-scene variability of atmospheric conditions. The surface reflectance algorithm uses ancillary data for water vapor and atmospheric ozone concentrations, as well as estimating atmospheric aerosols. Therefore, it could account for the within-scene variability under atmospheric conditions that cause problems for the image-to-image calibration.

In the path 76 swath acquired 31 July 2002 (Figure 3, panel 3), atmospheric conditions clearly varied within a single image swath. Thin clouds occurred in the northern portion of the swath, ranging from opaque (a) to translucent (b). Over the foothills and mountains the atmosphere was clearer (c), with spatially varying, translucent haze in the northern portion of the lowlands south of the mountains (d). Finally, the atmosphere appears extremely clear in the southern portion of the lowlands (e). A variable atmosphere like this poses problems for the image-to-image calibration method. While it might be possible to break the scene into sections which are calibrated separately, or develop spatially variable correction parameters, this was not attempted. Instead, the path 76 swath was calibrated mainly using the central portion of the scene (c). The results from the LEDAPS surface reflectance algorithm (Figure 3, panel 6) demonstrate that the surface reflectance algorithm was visually successful at mitigating many of the image defects caused by the variable atmospheric conditions.

Surface reflectance is more tightly related to vegetation properties, and is more likely to be directly comparable to on the ground spectral measurements and other remote sensing surface reflectance products such as the weekly eMODIS composites. Figure 4 compares three swaths processed to top-of-atmsophere reflectance and calibrated (panel 1) and processed to surface reflectance (panel 2) with the eMODIS weekly composite product from the same time period as the Landsat swaths. For this comparison, the same fixed contrast stretch parameters (stretched from 0 to 0.25 reflectance in the red, green, and blue bands) are used for all the images. It is clear that the Landsat surface reflectance product is much closer to the radiometry of the eMODIS product (panel 3).

Image differencing was used to assess the similarity of the spectral values from the two radiometric normalization approaches. In Figure 5, the reflectance difference between Path 78 (29 July 2002) and Path 76 (31 July 2002) was computed. In the top panels, the difference between calibrated top-of-atmsophere reflectance is presented. In the visible bands (1–3) there is a strong gradient from north (a) to south (b), with the Path 76 top-of-atmosphere reflectance higher than Path 78 in the north, and the reverse in the south. The apparent variations in atmospheric conditions in Path 76 discussed above have an effect on the computed difference between the swaths when a radiometric calibration is applied to the whole swath. The haze in Path 76 (c) results in higher reflectance in the visible bands with the image-to-image calibration approach. The abrupt horizontal breaks (d, e) occur between different scenes within a Landsat swath, and are an artifact of applying the solar elevation of the scene center to the whole scene. This results in artificial steps between scenes when in reality the solar elevation varies smoothly along the Landsat swath track. For the infrared bands (4, 5 and 7) the north-to-south gradient is absent, and the shadows from

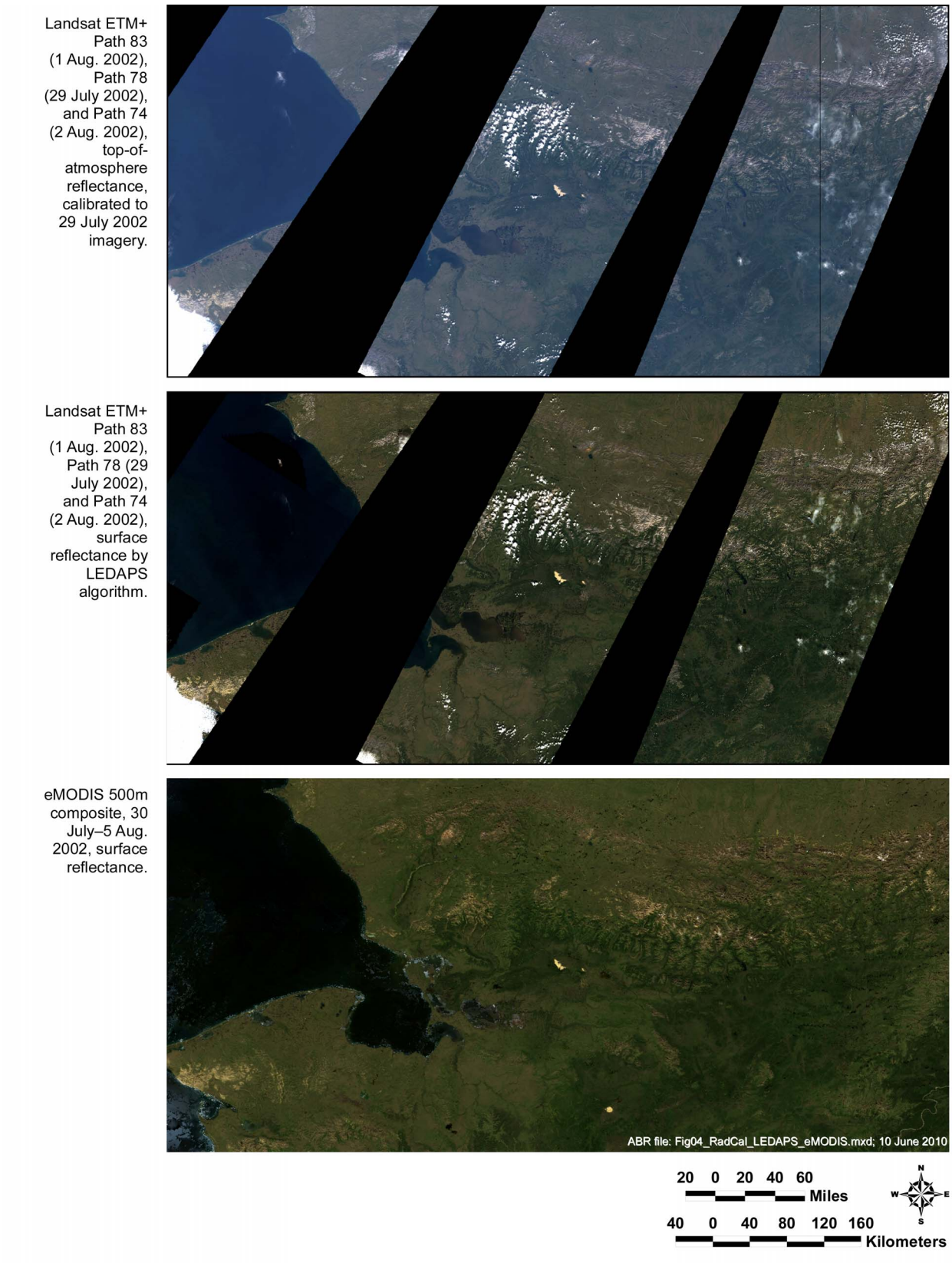


Figure 4. Visual comparison of Landsat Top-of-Atmosphere Reflectance, Landsat Surface Reflectance, and eMODIS Surface Reflectance.

Top-of-Atmosphere Reflectance, Image-to-Image Calibration to Path 78, 29 July 2002

Surface Reflectance by LEDAPS Algorithm

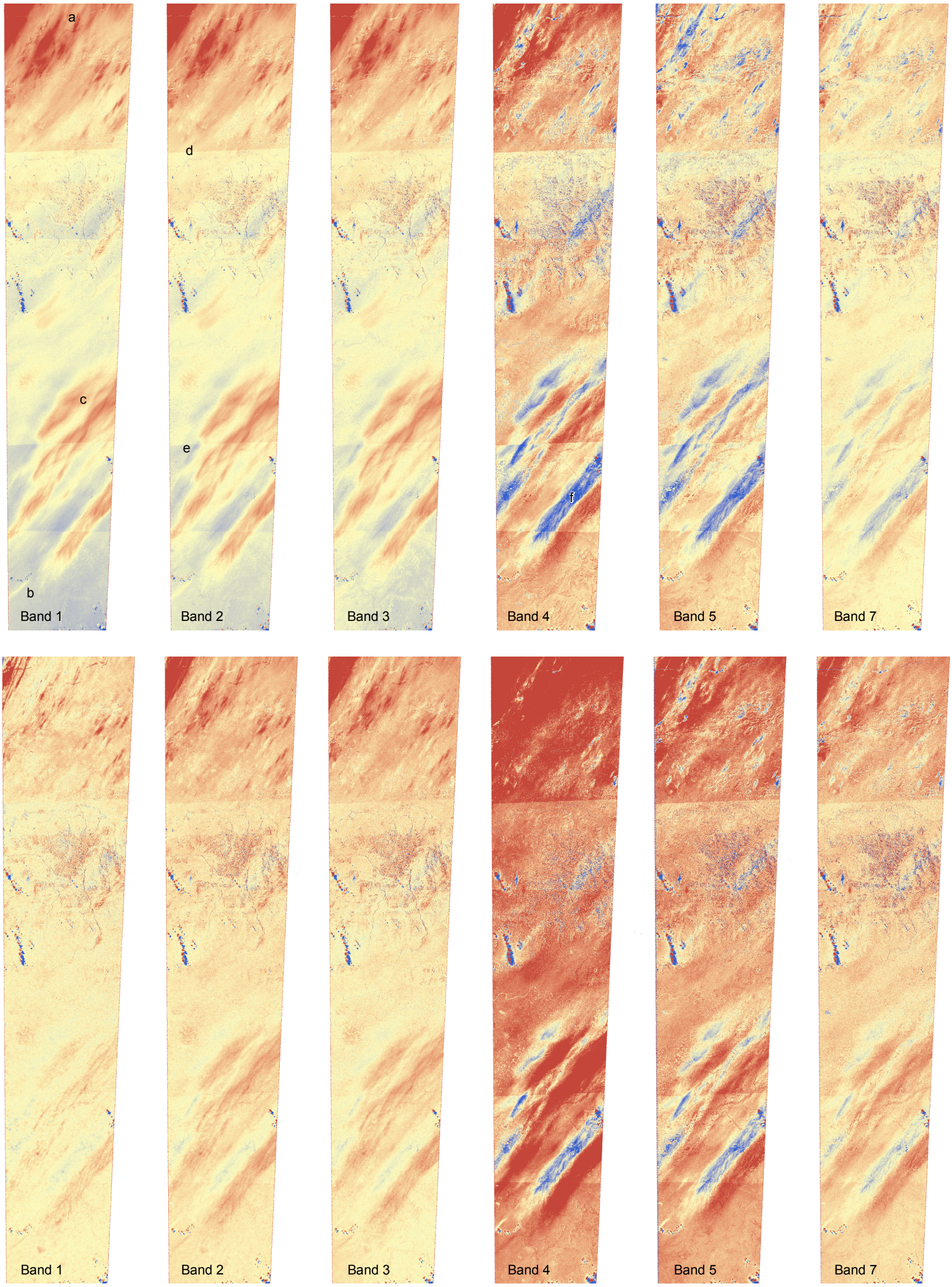
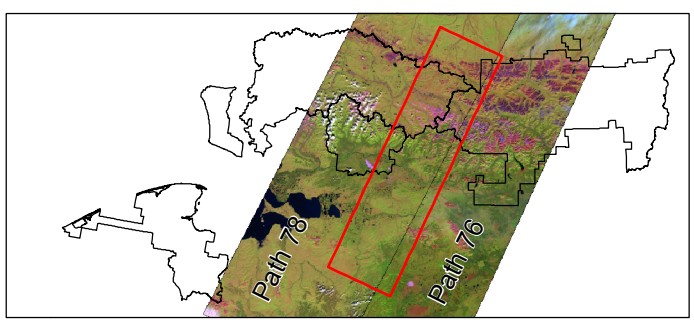


Figure 5. Reflectance Difference in Overlapping Portion of Landsat Swaths with Two Radiometric Normalization Approaches: Path 78 (29 July 2002) and Path 76 (31 July 2002).



ABR file: Fig05_RadCal_vs_LEDAPS_p78p76.mxd; 10 June 2010

Reflectance Difference

High : 0.025

Low : -0.025

Difference calculated from Path 78 (29 July 2002) minus Path 76 (31 July 2002).

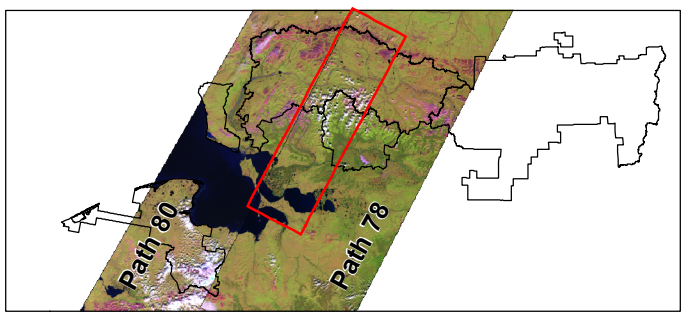
Top-of-Atmosphere Reflectance, Image-to-Image Calibration to Path 78, 29 July 2002

Band 1 | Band 2 | Band 3 | Band 4 | Band 5 | Band 7

Surface Reflectance by LEDAPS Algorithm

Band 1 | Band 2 | Band 3 | Band 4 | Band 5 | Band 7

Figure 6. Reflectance Difference in Overlapping Portion of Landsat Swaths with Two Radiometric Normalization Approaches: Path 78 (29 July 2002) and Path 80 (27 July 2002).



ABR file: Fig06_RadCal_vs_LEDAPS_p78p80.mxd; 10 June 2010

Reflectance Difference

High : 0.025

Low : -0.025

Difference calculated from Path 78 (29 July 2002) minus Path 80 (27 July 2002).

the haze are also much more pronounced (f).

The difference between surface reflectance for Path 78 and Path 76 is presented in the bottom panels of Figure 5. For the visible bands the north-to-south gradient is absent, and the effects of the haze are much reduced. However, the infrared values are consistently higher in Path 76, and the artifacts from the haze are very evident.

The difference between Path 78 (29 July 2002) and Path 80 (27 July 2002) is presented in Figure 6. The top panels compare the difference between calibrated top-of-atmsophere reflectance for the two swaths. The large differences near the center of the overlap area (a) are caused by clouds and cloud shadows in the Path 78 swath. For the rest of the area, the radiometry is very similar between the two swaths. The bottom panels compare the difference between surface reflectance for the two swaths. Generally, surface reflectance is higher for Path 80, especially in the infrared bands (4, 5 and 7).

The image differencing for two swath pairs suggests that, especially in the infrared bands, the eastern portion of swaths have higher reflectance than the western portion of swaths. The image-to-image calibration coefficients indicated the same pattern. This pattern could be related to the difference in sun/sensor geometry between the eastern and western edges of Landsat swaths. Landsat sensors are normally treated as nadir (vertical) viewing, but actually have a 15º field of view, with viewing angles departing up to 7.5º from nadir at the west and east edges of the scenes. As part of the WELD project, Roy and colleagues (2010b) used contemporaneous MODIS products to perform both atmospheric correction and radiometric normalization of Landsat imagery. They demonstrated that the mean Band 4 reflectance increased by 0.0017 for each degree of increase in the viewing angle from west to east for July 2008 Landsat imagery in the continental United States. This increase of approximately 0.025 across a full 15º would explain much of the difference between the overlapping regions of the swaths. This finding also challenges the soundness of the image-to-image radiometric calibration approach. A systematic positive bias in reflectance values for the eastern portion of swaths, and a negative bias for western portions, will result in a systematic drift in reflectance values across the extent of a mosaic calibrated using the image-to-image method.

Mosaicking

The surface reflectance correction method of radiometric calibration was used to produce the Landsat mosaics for the full study area. The surface reflectance algorithm successfully reduced the effect of haze and better accounted for atmospheric conditions that varied across a swath. Image differencing indicated that the differences were often larger with the surface reflection method than with the image-to-image calibration, particularly for the infrared bands; however, this could be largely explained by the subtle increase in reflectance values from the western to the eastern edge of each scene due to the slight off-nadir viewing angle of the Landsat satellite. Finally, the surface reflectance approach results in Landsat data that is more directly comparable to ground measurements and eMODIS or other remote sensing products.

Mosaics were constructed for three eras: 1999, 2002, and Alternate. The final mosaic which covered the full study area (excepting deep ocean portions) was constructed by selecting one of the three eras. Generally, 2002 data were preferred except where the 2002 data quality was poor due to clouds, cloud shadows, or thick haze.

The final mosaic (Figure 7) includes high-quality, nearly cloud-free data for the entire full study area excepting portions of the oceans. The six 30-m reflective Landsat bands (1, 2, 3, 4, 5 and 7) are the first six bands of the Erdas Imagine format file. The bands represent surface reflectance and are scaled by 10,000. The valid data values are between -2000 and 14,000; saturated values (where the digital number in the original imagery was 255) are stored as 16,000; and fill values are stored as -9999. The seventh band in the Imagine file is the aerosol optical thickness, as estimated by the LEDAPS algorithm. The eighth band is the solar zenith angle and the ninth band is the solar azimuth angle.

An ancillary layer, in both vector and raster format, provides the source swath that contributed to each portion of the mosaic (Figure 8). The date, day of year, and sensor are included as attributes and the mosaic area can be summarized for these different variables. 79.3% of the mosaic area was contributed by 2002 imagery from the three-week period between 18 July and 7 August 2002. 18.9% was contributed by 1999 imagery, 1.6% from other years, and 0.2% from other dates in 2002.

DEM Preprocessing

The NED and G-DEM data for the full study area were acquired and processed to 30-m resolution. The G-DEM was more detailed and appeared to better represent the location of some sharp features such as ridgelines. However, review of the hillshades (Figure 9) indicated substantial occurrence of artifacts that would cause misrepresentation of the solar incidence angle. This would in turn cause errors in the topographic normalization. The NED DEM was much smoother and there were few severe artifacts. There were cases of ridgelines that were not well-aligned with the Landsat data; these would cause errors in the topographic normalization because the DEM might cause bright sunlit slopes to be corrected as if they were shadowed. Due to the lower severity of the visible artifacts, the NED DEM was selected as the basis for the topographic normalization.

Topographic Normalization

The stratified sample data for developing the topographic normalization was subsampled using different ranges of slope and NDVI. For each subset, 10 linear regression trials were performed with $\ln(\rho_T \cos e)$ as the dependent variable and $\ln(\cos e \cos i)$ as the dependent variable; each trial randomly selected 10% of the samples. The slope of the regression line was an estimate of the k value for that band and that range of NDVI and slope.

The regressions consistently demonstrated strong relationships ($r^2 > 0.1$) and consistent k values (standard deviation of k values < 0.10 from the multiple trials) for Minnaert k estimation for many, but not all, of the slope and NDVI subsets. Subsets of data characterized by moderate slopes (10–45 degrees) and across a wide range of NDVI (~0.15–0.90) had strong and consistent estimates of k. For lower slopes (approaching flat terrain) the patterns were not as consistent, probably due to the narrow range of variability of the solar incidence and slope. For slopes higher than 45 degrees, some of the subsets had consistent relationships but most did not. The sample sizes for many combinations of slope and NDVI were very small, and slopes greater than 45 degrees comprised 0.0768% of the full study area. NDVI values less than 0.15 were usually deep shadow, water, snow, or partially snow-covered. NDVI values > 0.90 frequently occurred in broadleaf forests but also occurred (spuriously) over water, when very low band 4 values were higher than very low band 3 values.

The mean Minnaert k values were summarized by band, slope bin (1 degree bins ranging from 10–45 degrees), and NDVI bin (NDVI values between 0.05

Landsat Mosaic c. 2002

False Color (5/4/3)

Arctic Park Network

Approximate scale = 1:2,250,000

10 0 10 20 30 Miles

10 0 10 20 30 40 Kilometers

N W E S

Data from 30 Landsat swaths, primarily acquired between 18 July and 7 August 2002. Processed to surface reflectance and mosaicked to remove clouds and cloud shadows.

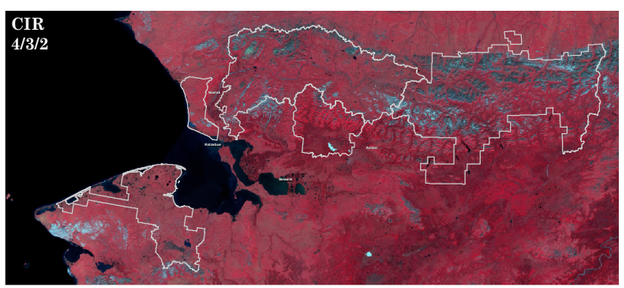
Map projection: Albers Alaska, NAD 83, meters.
30-m pixels, 13290 rows by 29812 columns.

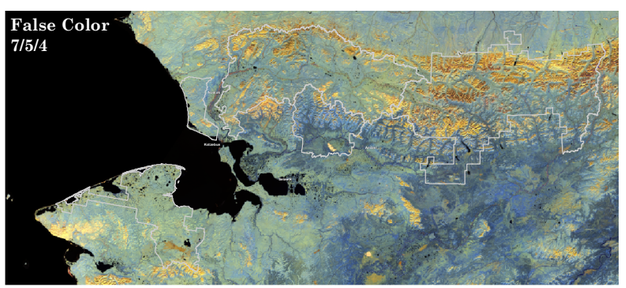
Noatak
Kotzebue
Shishmaref
Selawik
Ambler
Anaktuvak Pass

170°0'0"W 169°0'0"W 168°0'0"W 167°0'0"W 166°0'0"W 165°0'0"W 164°0'0"W 163°0'0"W 162°0'0"W 161°0'0"W 160°0'0"W 159°0'0"W 158°0'0"W 157°0'0"W 156°0'0"W 155°0'0"W 154°0'0"W 153°0'0"W 152°0'0"W 151°0'0"W 150°0'0"W

69°0'0"N 68°30'0"N 68°0'0"N 67°30'0"N 67°0'0"N 66°30'0"N 66°0'0"N 65°30'0"N 65°0'0"N







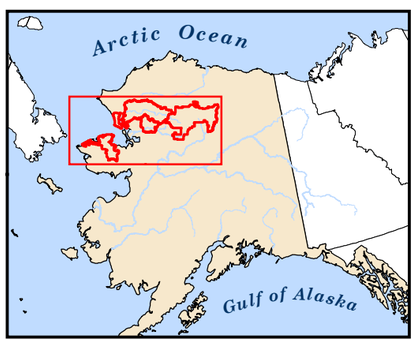


Figure 7: Arctic Park Network Landsat Mosaic, circa 2002.

ABR file: Fig07_LandsatMosaic.mxd; 10 June 2010

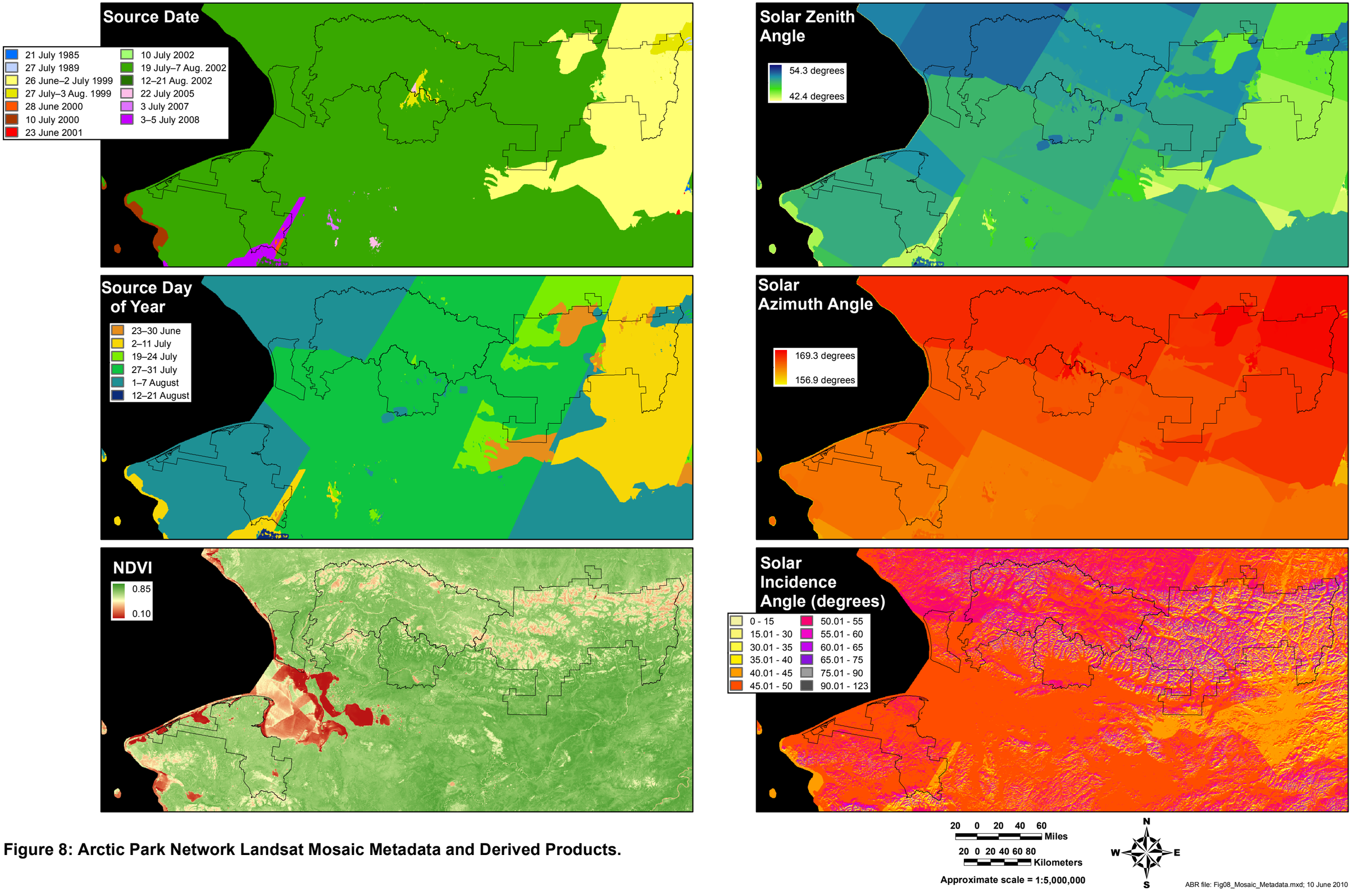


Figure 8: Arctic Park Network Landsat Mosaic Metadata and Derived Products.

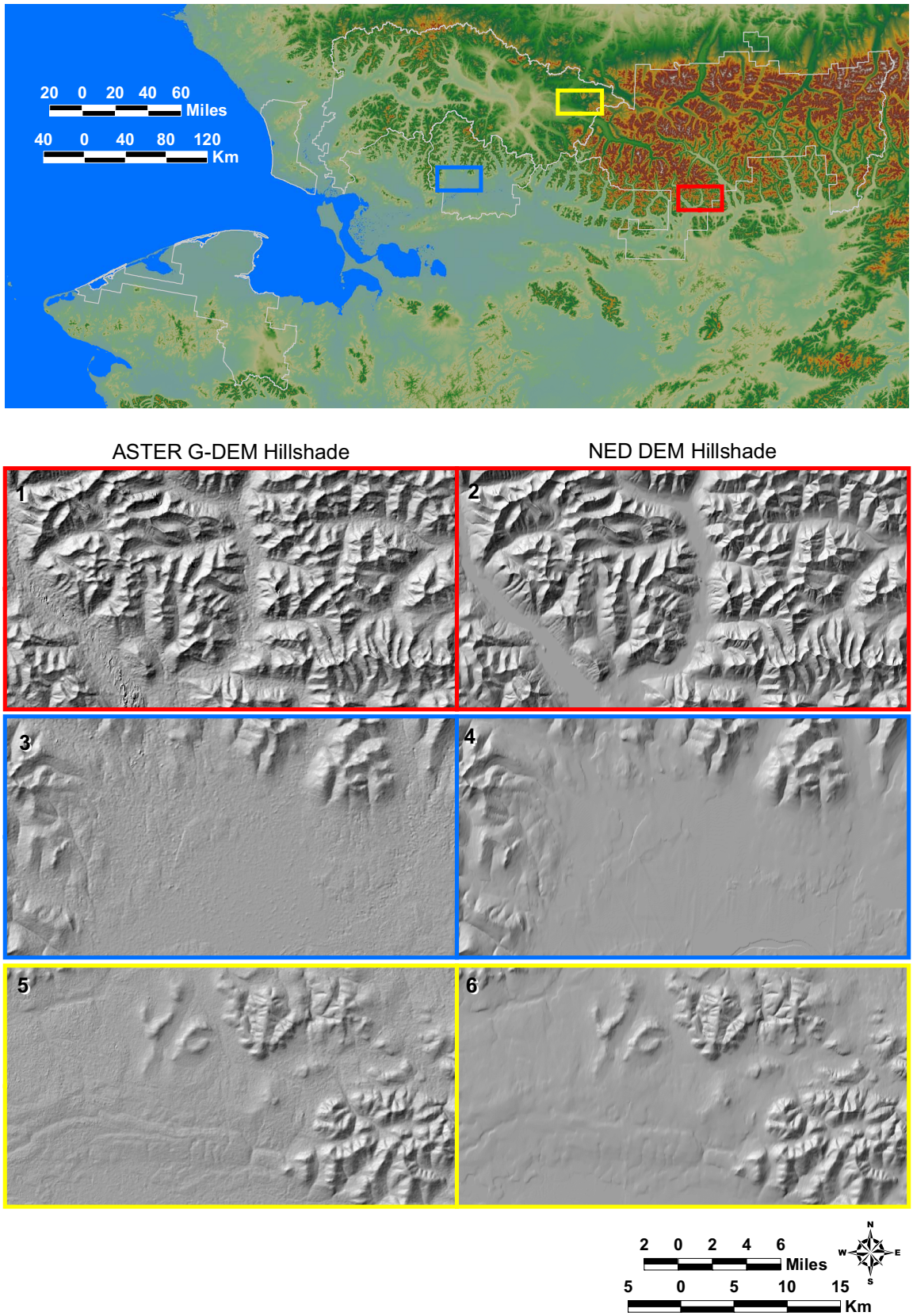


Figure 9. Visual Comparison of Hillshades from ASTER G-DEM and NED DEM.

and 0.85 were rounded to the nearest tenth unit of NDVI). These values are summarized in Tables 9–14 for Landsat TM/ETM+ bands 1, 2, 3, 4, 5 and 7, respectively. Data beyond the bounds of the *k* values was assigned by extending the range of the slope and NDVI bins at the edges. For example, the *k* value developed for a slope of 10 degrees was extended to cover the remaining slope range (slopes of 0–9 degrees). This approach provided a defined *k* value for all combinations of slope and NDVI based on the *k* values established with confidence. Improvements in the method of assigning appropriate *k* values when the regression relationship is not strong are left to future research.

For all bands, *k* increased with wavelength, with the lowest *k* values for band 1 and the highest for band 7. In all bands, *k* decreased with NDVI. The effect of slope was modest, especially for the visible bands 1 and 2. *k* values usually increased with slope initially, then decreased beyond some threshold that varied by band and NDVI bin.

The *k* values from tables 9–14, in combination with the slope and NDVI layers, were used to generate *k* images for each band. These were then used to generate the correction factor images, and the topographically normalized mosaic (Figure 10). The normalization visibly improved the image in areas of moderate topography. There were problems associated with misalignments of the DEM used for the correction, which were most pronounced near ridgelines. The topographic normalization equation was not defined for terrain with solar incidence angles greater than 90 degrees (i.e., slopes facing away from the sun), and pixels in those areas were assigned fill values. Very high solar incidence angles (75–80 degrees and higher) had visibly poor results in many cases, perhaps due to the extensive shadowing. The topographically normalized mosaic was not assessed quantitatively, but methods to assess it could include plotting profiles across areas with homogeneous vegetation but variable illumination.

Conclusions

A cloud-free, surface reflectance calibrated Landsat mosaic was produced. The mosaic covers all of the Arctic Network Parks and surrounding areas, and is composed primarily from data acquired during a three-week period in late summer 2002. An efficient process for reviewing, ingesting, and calibrating Landsat data was developed; the scripts used for the processing are included with the deliverable and are described in Appendix 1. Newer or older scenes processed using the same approach may be directly compared to the c. 2002 mosaic, either visually or using image differencing and other time-series techniques. Due to the scan-line corrector malfunction on Landsat 7 and the limited duty cycle of Landsat 5, it is unlikely that a similar mosaic can be constructed for the current era; however, data for portions of parks may easily be collected. The best opportunity to collect an updated mosaic will come after the launch of the Landsat Data Continuity Mission, which is currently scheduled for December 2012.

Table 9. Landsat TM/ETM+ band 1 Minnaert k values as a function of slope and NDVI.

Slope	-0.4000–2500	0.2501–0.3500	0.3501–0.4500	0.4501–0.5500	0.5501–0.6500	0.6501–0.7500	0.7501–1.0000	Mean	Range
0–10	0.884	0.705	0.681	0.633	0.565	0.489	0.483	0.635	0.401
11	0.704	0.716	0.695	0.649	0.575	0.503	0.490	0.619	0.226
12	0.701	0.716	0.698	0.665	0.593	0.505	0.506	0.626	0.211
13	0.690	0.719	0.692	0.660	0.612	0.522	0.504	0.628	0.215
14	0.695	0.713	0.685	0.665	0.631	0.534	0.512	0.634	0.201
15	0.709	0.712	0.679	0.674	0.631	0.541	0.505	0.636	0.208
16	0.686	0.699	0.691	0.666	0.634	0.546	0.512	0.633	0.187
17	0.692	0.690	0.684	0.670	0.631	0.559	0.511	0.634	0.180
18	0.702	0.685	0.680	0.663	0.628	0.553	0.501	0.630	0.201
19	0.687	0.675	0.680	0.663	0.629	0.552	0.493	0.626	0.194
20	0.695	0.662	0.670	0.658	0.626	0.556	0.487	0.622	0.208
21	0.700	0.654	0.662	0.648	0.628	0.554	0.483	0.619	0.218
22	0.684	0.653	0.658	0.649	0.628	0.554	0.486	0.616	0.198
23	0.659	0.651	0.652	0.644	0.628	0.550	0.470	0.608	0.189
24	0.646	0.657	0.648	0.634	0.621	0.550	0.477	0.605	0.179
25	0.624	0.642	0.648	0.636	0.618	0.554	0.469	0.599	0.179
26	0.615	0.650	0.649	0.634	0.615	0.550	0.466	0.597	0.185
27	0.585	0.647	0.647	0.630	0.608	0.544	0.465	0.590	0.182
28	0.597	0.649	0.643	0.630	0.600	0.535	0.456	0.587	0.193
29	0.608	0.648	0.651	0.625	0.599	0.529	0.451	0.587	0.200
30	0.615	0.648	0.646	0.624	0.593	0.527	0.452	0.586	0.196
31	0.630	0.652	0.648	0.615	0.585	0.522	0.449	0.586	0.203
32	0.644	0.654	0.647	0.615	0.585	0.528	0.461	0.591	0.193
33	0.643	0.645	0.641	0.610	0.582	0.529	0.458	0.587	0.187
34	0.633	0.649	0.642	0.614	0.575	0.528	0.461	0.586	0.188
35	0.643	0.657	0.646	0.606	0.570	0.528	0.459	0.587	0.198
36	0.644	0.662	0.652	0.617	0.577	0.525	0.452	0.590	0.210
37	0.649	0.667	0.649	0.614	0.576	0.525	0.452	0.590	0.215
38	0.675	0.684	0.671	0.622	0.575	0.517	0.440	0.598	0.245
39	0.699	0.698	0.668	0.627	0.580	0.513	0.434	0.603	0.265
40	0.716	0.696	0.679	0.642	0.582	0.512	0.432	0.609	0.284
41	0.722	0.709	0.674	0.641	0.585	0.510	0.436	0.611	0.287
42	0.707	0.730	0.683	0.647	0.587	0.505	0.429	0.612	0.301
43	0.710	0.724	0.689	0.660	0.577	0.495	0.434	0.613	0.290
44	0.698	0.735	0.673	0.649	0.592	0.509	0.416	0.610	0.319
45–77	0.685	0.726	0.659	0.639	0.588	0.546	0.434	0.611	0.292
Mean	0.674	0.680	0.666	0.640	0.600	0.531	0.467	0.608	0.213
Range	0.299	0.093	0.057	0.069	0.068	0.069	0.096	0.050	0.468

Table 10. Landsat TM/ETM+ band 2 Minnaert k values as a function of slope and NDVI.

Slope	-0.4000–2500	0.2501–0.3500	0.3501–0.4500	0.4501–0.5500	0.5501–0.6500	0.6501–0.7500	0.7501–1.0000	Mean	Range
0–10	0.884	0.777	0.729	0.650	0.548	0.465	0.455	0.644	0.429
11	0.782	0.793	0.759	0.673	0.562	0.485	0.479	0.647	0.314
12	0.779	0.794	0.763	0.698	0.589	0.511	0.511	0.664	0.283
13	0.766	0.791	0.753	0.698	0.613	0.533	0.517	0.667	0.274
14	0.768	0.786	0.744	0.705	0.637	0.550	0.542	0.676	0.244
15	0.782	0.788	0.746	0.717	0.643	0.555	0.534	0.681	0.254
16	0.761	0.775	0.758	0.714	0.653	0.567	0.547	0.682	0.228
17	0.765	0.772	0.755	0.718	0.652	0.574	0.549	0.684	0.223
18	0.776	0.766	0.753	0.716	0.650	0.576	0.548	0.684	0.229
19	0.764	0.758	0.752	0.721	0.655	0.578	0.540	0.681	0.224
20	0.774	0.746	0.748	0.716	0.659	0.586	0.538	0.681	0.236
21	0.776	0.738	0.737	0.710	0.663	0.585	0.536	0.678	0.241
22	0.760	0.734	0.734	0.712	0.668	0.588	0.542	0.677	0.219
23	0.736	0.733	0.728	0.710	0.672	0.588	0.534	0.672	0.202
24	0.721	0.739	0.721	0.702	0.666	0.590	0.543	0.669	0.196
25	0.699	0.724	0.720	0.704	0.669	0.601	0.548	0.666	0.176
26	0.688	0.727	0.719	0.700	0.673	0.603	0.547	0.665	0.179
27	0.662	0.726	0.716	0.699	0.671	0.605	0.551	0.661	0.175
28	0.668	0.726	0.716	0.701	0.664	0.606	0.543	0.661	0.183
29	0.682	0.724	0.726	0.698	0.666	0.603	0.543	0.663	0.183
30	0.688	0.722	0.719	0.697	0.660	0.600	0.537	0.661	0.185
31	0.701	0.729	0.722	0.689	0.650	0.591	0.537	0.660	0.193
32	0.714	0.731	0.721	0.688	0.651	0.595	0.543	0.664	0.188
33	0.712	0.721	0.713	0.680	0.643	0.586	0.533	0.655	0.187
34	0.703	0.723	0.711	0.681	0.636	0.584	0.528	0.652	0.195
35	0.711	0.733	0.711	0.672	0.629	0.581	0.526	0.652	0.207
36	0.708	0.732	0.713	0.679	0.634	0.581	0.519	0.652	0.214
37	0.712	0.733	0.706	0.684	0.630	0.581	0.519	0.652	0.215
38	0.734	0.747	0.728	0.678	0.627	0.572	0.505	0.656	0.242
39	0.754	0.757	0.727	0.681	0.632	0.570	0.503	0.661	0.255
40	0.769	0.752	0.737	0.690	0.627	0.564	0.499	0.663	0.270
41	0.772	0.762	0.733	0.692	0.632	0.563	0.497	0.664	0.275
42	0.756	0.785	0.744	0.694	0.627	0.559	0.494	0.666	0.291
43	0.756	0.784	0.749	0.705	0.618	0.541	0.489	0.663	0.295
44	0.744	0.793	0.731	0.704	0.635	0.567	0.481	0.665	0.312
45–77	0.733	0.784	0.713	0.683	0.628	0.567	0.487	0.657	0.296
Mean	0.741	0.753	0.732	0.696	0.640	0.571	0.524	0.665	0.229
Range	0.222	0.073	0.057	0.071	0.124	0.140	0.096	0.040	0.429

Table 11. Landsat TM/ETM+ band 3 Minnaert k values as a function of slope and NDVI.

Slope	-0.4000–2500	0.2501–0.3500	0.3501–0.4500	0.4501–0.5500	0.5501–0.6500	0.6501–0.7500	0.7501–1.0000	Mean	Range
0–10	0.884	0.815	0.752	0.669	0.556	0.486	0.518	0.668	0.399
11	0.831	0.840	0.790	0.698	0.573	0.508	0.546	0.684	0.332
12	0.827	0.839	0.796	0.721	0.604	0.537	0.585	0.701	0.302
13	0.819	0.835	0.791	0.728	0.631	0.568	0.599	0.710	0.267
14	0.818	0.835	0.787	0.736	0.658	0.586	0.625	0.721	0.248
15	0.837	0.838	0.792	0.753	0.666	0.591	0.620	0.728	0.247
16	0.816	0.824	0.804	0.751	0.683	0.607	0.631	0.731	0.218
17	0.823	0.828	0.803	0.758	0.683	0.614	0.633	0.734	0.214
18	0.838	0.825	0.803	0.756	0.682	0.617	0.631	0.736	0.221
19	0.825	0.818	0.804	0.764	0.692	0.623	0.626	0.736	0.202
20	0.836	0.808	0.801	0.759	0.697	0.633	0.622	0.737	0.214
21	0.840	0.800	0.794	0.755	0.705	0.633	0.619	0.735	0.221
22	0.826	0.796	0.790	0.761	0.712	0.640	0.625	0.736	0.201
23	0.800	0.799	0.783	0.758	0.717	0.644	0.616	0.731	0.184
24	0.784	0.805	0.776	0.753	0.714	0.648	0.626	0.730	0.179
25	0.761	0.789	0.776	0.757	0.718	0.659	0.627	0.727	0.161
26	0.751	0.795	0.776	0.754	0.725	0.661	0.629	0.727	0.166
27	0.725	0.794	0.774	0.755	0.726	0.666	0.633	0.725	0.161
28	0.730	0.792	0.777	0.758	0.722	0.669	0.624	0.725	0.169
29	0.744	0.792	0.791	0.756	0.726	0.668	0.627	0.729	0.165
30	0.752	0.790	0.782	0.754	0.723	0.666	0.621	0.727	0.169
31	0.765	0.795	0.787	0.749	0.711	0.657	0.620	0.726	0.175
32	0.778	0.798	0.785	0.745	0.712	0.661	0.624	0.729	0.174
33	0.776	0.782	0.773	0.736	0.700	0.649	0.620	0.719	0.163
34	0.766	0.787	0.768	0.737	0.690	0.646	0.611	0.715	0.176
35	0.771	0.797	0.768	0.724	0.683	0.645	0.610	0.714	0.187
36	0.767	0.795	0.768	0.728	0.689	0.643	0.603	0.713	0.192
37	0.768	0.793	0.757	0.733	0.689	0.643	0.603	0.712	0.190
38	0.791	0.808	0.785	0.731	0.683	0.630	0.588	0.716	0.220
39	0.810	0.819	0.784	0.734	0.687	0.628	0.585	0.721	0.234
40	0.824	0.810	0.792	0.745	0.684	0.624	0.583	0.723	0.241
41	0.824	0.823	0.787	0.746	0.685	0.619	0.582	0.724	0.242
42	0.802	0.842	0.797	0.745	0.680	0.619	0.578	0.723	0.265
43	0.801	0.843	0.796	0.755	0.672	0.596	0.569	0.719	0.274
44	0.791	0.849	0.775	0.762	0.691	0.633	0.552	0.722	0.297
45–77	0.779	0.845	0.758	0.735	0.691	0.633	0.564	0.715	0.280
Mean	0.797	0.812	0.784	0.743	0.685	0.624	0.605	0.721	0.207
Range	0.160	0.067	0.052	0.095	0.170	0.183	0.116	0.068	0.399

Table 12. Landsat TM/ETM+ band 4 Minnaert k values as a function of slope and NDVI.

Slope	-0.4000–2500	0.2501–0.3500	0.3501–0.4500	0.4501–0.5500	0.5501–0.6500	0.6501–0.7500	0.7501–1.0000	Mean	Range
0–10	0.884	0.816	0.757	0.661	0.558	0.512	0.548	0.677	0.373
11	0.828	0.843	0.797	0.689	0.580	0.530	0.566	0.691	0.313
12	0.822	0.839	0.803	0.714	0.609	0.554	0.603	0.706	0.286
13	0.816	0.837	0.797	0.722	0.633	0.584	0.614	0.715	0.253
14	0.816	0.840	0.790	0.733	0.660	0.599	0.636	0.725	0.241
15	0.833	0.841	0.795	0.748	0.664	0.605	0.627	0.730	0.236
16	0.813	0.828	0.807	0.750	0.678	0.619	0.633	0.733	0.208
17	0.817	0.832	0.804	0.757	0.681	0.630	0.635	0.737	0.202
18	0.834	0.830	0.803	0.757	0.680	0.630	0.641	0.739	0.204
19	0.821	0.821	0.806	0.764	0.691	0.635	0.628	0.738	0.193
20	0.832	0.810	0.802	0.758	0.694	0.644	0.629	0.738	0.203
21	0.835	0.804	0.794	0.755	0.702	0.644	0.623	0.737	0.212
22	0.822	0.800	0.790	0.761	0.711	0.650	0.630	0.738	0.192
23	0.796	0.803	0.784	0.759	0.713	0.652	0.620	0.732	0.183
24	0.782	0.808	0.775	0.754	0.710	0.654	0.625	0.730	0.182
25	0.759	0.792	0.776	0.758	0.714	0.668	0.632	0.728	0.160
26	0.748	0.797	0.775	0.755	0.722	0.670	0.631	0.728	0.166
27	0.722	0.795	0.772	0.757	0.722	0.673	0.635	0.725	0.159
28	0.728	0.793	0.776	0.759	0.719	0.676	0.630	0.726	0.163
29	0.742	0.793	0.790	0.758	0.723	0.670	0.631	0.730	0.162
30	0.749	0.791	0.780	0.755	0.722	0.671	0.621	0.727	0.169
31	0.763	0.796	0.786	0.751	0.710	0.660	0.621	0.727	0.175
32	0.775	0.799	0.785	0.744	0.713	0.663	0.621	0.729	0.178
33	0.773	0.784	0.773	0.736	0.699	0.653	0.614	0.719	0.170
34	0.765	0.787	0.766	0.737	0.692	0.646	0.607	0.714	0.180
35	0.770	0.799	0.767	0.724	0.686	0.645	0.605	0.714	0.194
36	0.766	0.795	0.766	0.728	0.689	0.647	0.599	0.713	0.196
37	0.766	0.795	0.758	0.734	0.685	0.647	0.599	0.712	0.196
38	0.791	0.811	0.782	0.731	0.682	0.634	0.572	0.715	0.239
39	0.809	0.822	0.783	0.733	0.684	0.633	0.569	0.719	0.253
40	0.822	0.814	0.792	0.743	0.682	0.629	0.566	0.721	0.256
41	0.825	0.824	0.786	0.746	0.685	0.620	0.561	0.721	0.264
42	0.803	0.842	0.798	0.747	0.681	0.620	0.564	0.722	0.278
43	0.802	0.841	0.796	0.757	0.675	0.602	0.552	0.718	0.289
44	0.794	0.847	0.776	0.763	0.692	0.634	0.538	0.721	0.309
45–77	0.782	0.843	0.755	0.737	0.692	0.634	0.539	0.712	0.303
Mean	0.795	0.814	0.785	0.743	0.684	0.632	0.605	0.722	0.209
Range	0.162	0.063	0.052	0.103	0.165	0.164	0.103	0.063	0.373

Table 13. Landsat TM/ETM+ band 5 Minnaert k values as a function of slope and NDVI.

Slope	-0.4000–2500	0.2501–0.3500	0.3501–0.4500	0.4501–0.5500	0.5501–0.6500	0.6501–0.7500	0.7501–1.0000	Mean	Range
0–10	0.884	0.854	0.829	0.752	0.656	0.639	0.653	0.752	0.245
11	0.916	0.898	0.862	0.777	0.674	0.656	0.674	0.780	0.259
12	0.930	0.888	0.869	0.797	0.703	0.679	0.714	0.797	0.251
13	0.933	0.898	0.859	0.803	0.732	0.708	0.725	0.808	0.225
14	0.932	0.911	0.853	0.818	0.757	0.718	0.749	0.820	0.214
15	0.942	0.913	0.862	0.828	0.760	0.717	0.737	0.823	0.225
16	0.936	0.904	0.869	0.829	0.778	0.728	0.751	0.828	0.208
17	0.930	0.915	0.866	0.834	0.778	0.740	0.752	0.831	0.190
18	0.945	0.915	0.875	0.836	0.770	0.736	0.753	0.833	0.209
19	0.950	0.912	0.884	0.846	0.780	0.741	0.748	0.837	0.209
20	0.962	0.906	0.886	0.838	0.781	0.749	0.747	0.839	0.215
21	0.971	0.904	0.884	0.838	0.789	0.746	0.739	0.839	0.231
22	0.966	0.902	0.882	0.844	0.795	0.752	0.742	0.840	0.223
23	0.947	0.908	0.874	0.838	0.800	0.752	0.730	0.836	0.217
24	0.931	0.911	0.858	0.833	0.795	0.753	0.733	0.831	0.198
25	0.911	0.893	0.858	0.840	0.797	0.762	0.737	0.828	0.174
26	0.907	0.896	0.852	0.834	0.808	0.763	0.734	0.828	0.173
27	0.888	0.888	0.848	0.834	0.803	0.760	0.737	0.823	0.151
28	0.890	0.879	0.845	0.834	0.794	0.755	0.723	0.817	0.166
29	0.901	0.882	0.858	0.826	0.793	0.749	0.719	0.818	0.182
30	0.907	0.882	0.846	0.821	0.788	0.739	0.708	0.813	0.199
31	0.914	0.884	0.849	0.816	0.772	0.729	0.700	0.809	0.214
32	0.918	0.886	0.845	0.809	0.775	0.732	0.704	0.810	0.214
33	0.921	0.870	0.832	0.796	0.763	0.718	0.693	0.799	0.228
34	0.909	0.875	0.832	0.806	0.758	0.715	0.682	0.797	0.227
35	0.913	0.883	0.839	0.790	0.750	0.714	0.680	0.796	0.233
36	0.912	0.876	0.843	0.792	0.752	0.712	0.670	0.794	0.242
37	0.911	0.880	0.837	0.810	0.748	0.712	0.670	0.796	0.241
38	0.923	0.894	0.860	0.796	0.744	0.694	0.641	0.793	0.282
39	0.929	0.902	0.864	0.790	0.741	0.690	0.631	0.792	0.298
40	0.937	0.886	0.863	0.800	0.738	0.682	0.622	0.790	0.314
41	0.926	0.897	0.847	0.800	0.742	0.671	0.617	0.786	0.309
42	0.892	0.918	0.858	0.800	0.731	0.666	0.608	0.782	0.310
43	0.902	0.914	0.846	0.804	0.722	0.640	0.595	0.775	0.319
44	0.891	0.914	0.816	0.803	0.740	0.668	0.575	0.772	0.339
45–77	0.891	0.914	0.800	0.803	0.740	0.668	0.581	0.771	0.333
Mean	0.921	0.896	0.854	0.814	0.760	0.715	0.694	0.808	0.227
Range	0.086	0.064	0.086	0.094	0.152	0.124	0.178	0.088	0.396

Table 14. Landsat TM/ETM+ band 7 Minnaert k values as a function of slope and NDVI.

Slope	-0.4000–2500	0.2501–0.3500	0.3501–0.4500	0.4501–0.5500	0.5501–0.6500	0.6501–0.7500	0.7501–1.0000	Mean	Range
0–10	0.884	0.853	0.837	0.771	0.692	0.658	0.657	0.765	0.227
11	0.920	0.895	0.873	0.797	0.712	0.677	0.678	0.793	0.243
12	0.935	0.889	0.879	0.818	0.737	0.697	0.718	0.810	0.238
13	0.935	0.901	0.872	0.824	0.766	0.727	0.733	0.823	0.208
14	0.935	0.917	0.867	0.841	0.787	0.737	0.757	0.834	0.198
15	0.948	0.921	0.877	0.849	0.793	0.737	0.745	0.839	0.211
16	0.944	0.913	0.884	0.851	0.811	0.747	0.761	0.844	0.197
17	0.943	0.928	0.884	0.856	0.810	0.760	0.760	0.849	0.182
18	0.963	0.928	0.895	0.862	0.803	0.755	0.760	0.852	0.208
19	0.967	0.925	0.904	0.872	0.812	0.763	0.759	0.857	0.208
20	0.982	0.917	0.906	0.865	0.812	0.770	0.756	0.858	0.226
21	0.991	0.915	0.904	0.867	0.820	0.769	0.749	0.859	0.242
22	0.987	0.913	0.904	0.873	0.825	0.773	0.753	0.861	0.233
23	0.967	0.918	0.895	0.865	0.828	0.772	0.742	0.855	0.226
24	0.951	0.922	0.881	0.859	0.823	0.770	0.744	0.850	0.207
25	0.929	0.905	0.880	0.866	0.824	0.776	0.748	0.847	0.181
26	0.928	0.910	0.876	0.859	0.831	0.777	0.744	0.846	0.184
27	0.904	0.903	0.873	0.859	0.824	0.772	0.747	0.840	0.157
28	0.907	0.894	0.869	0.857	0.816	0.766	0.730	0.834	0.178
29	0.919	0.896	0.882	0.848	0.814	0.762	0.726	0.836	0.193
30	0.927	0.898	0.871	0.845	0.807	0.751	0.717	0.831	0.210
31	0.937	0.900	0.872	0.840	0.792	0.741	0.707	0.827	0.230
32	0.939	0.902	0.867	0.834	0.796	0.746	0.712	0.828	0.227
33	0.943	0.885	0.855	0.823	0.786	0.728	0.702	0.817	0.241
34	0.927	0.892	0.856	0.833	0.778	0.723	0.686	0.814	0.241
35	0.932	0.898	0.864	0.816	0.767	0.720	0.683	0.811	0.249
36	0.932	0.893	0.871	0.816	0.768	0.716	0.672	0.810	0.260
37	0.932	0.899	0.865	0.835	0.762	0.716	0.672	0.812	0.261
38	0.944	0.911	0.888	0.817	0.755	0.697	0.642	0.808	0.302
39	0.952	0.923	0.892	0.810	0.754	0.689	0.632	0.808	0.320
40	0.959	0.909	0.889	0.818	0.748	0.681	0.623	0.804	0.336
41	0.948	0.922	0.872	0.817	0.755	0.673	0.619	0.801	0.329
42	0.912	0.943	0.881	0.820	0.738	0.670	0.604	0.795	0.339
43	0.917	0.933	0.872	0.822	0.727	0.641	0.594	0.787	0.340
44	0.903	0.933	0.838	0.821	0.752	0.669	0.568	0.783	0.365
45–77	0.903	0.933	0.821	0.821	0.752	0.669	0.579	0.783	0.354
Mean	0.937	0.909	0.875	0.837	0.783	0.728	0.699	0.824	0.238
Range	0.106	0.090	0.084	0.102	0.139	0.136	0.192	0.097	0.422

Topographically Normalized Landsat Mosaic c. 2002

False Color (5/4/3)

Arctic Park Network

Approximate scale = 1:2,250,000

10 0 10 20 30 Miles

10 0 10 20 30 40 Kilometers

N W E S

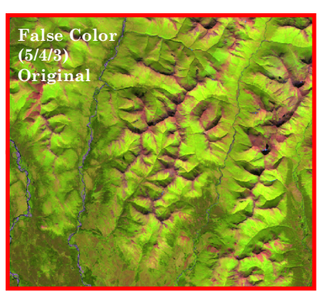
Data from 30 Landsat swaths, primarily acquired between 18 July and 7 August 2002. Minnaert correction applied using *k* values defined as a function of band, NDVI and slope.

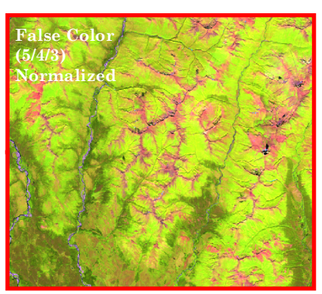
Map projection: Albers Alaska, NAD 83, meters. 30-m pixels, 13290 rows by 29812 columns.

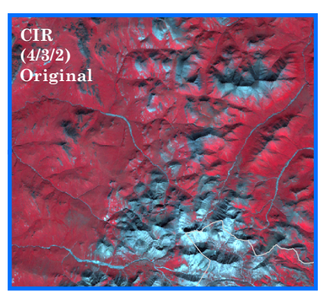
Noatak
Kotzebue
Shishmaref
Selawik
Ambler
Anaktuvak Pass

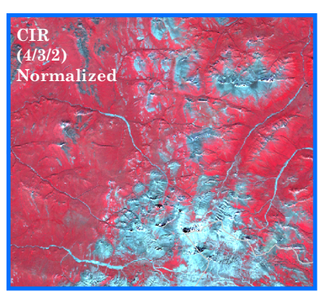
170°0'0"W 169°0'0"W 168°0'0"W 167°0'0"W 166°0'0"W 165°0'0"W 164°0'0"W 163°0'0"W 162°0'0"W 161°0'0"W 160°0'0"W 159°0'0"W 158°0'0"W 157°0'0"W 156°0'0"W 155°0'0"W 154°0'0"W 153°0'0"W 152°0'0"W 151°0'0"W 150°0'0"W

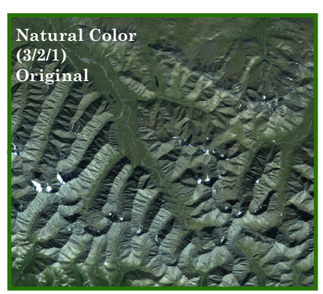
69°0'0"N 68°30'0"N 67°30'0"N 67°0'0"N 66°30'0"N 66°0'0"N 65°30'0"N 65°0'0"N











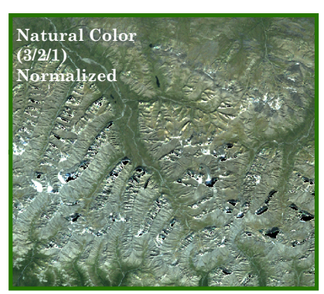




Figure 10. Topographically Normalized Landsat Mosaic, circa 2002.

ABR file: Fig10_Topographic_Normalization.mxd; 11 June 2010

Appendix 1: Data Deliverable Overview

Ancillary\Clouds: Subfolders are organized by WRS2 path. Within each subfolder, the rough outlines of cloud-affected areas are stored in shapefiles for each swath, along with a text file listing the WRS2 rows that the cloud mask applies to. The shapefile and text file, if present, are referenced by the *Scripts\02_raw\new_landsat_processing\new_landsat_processing.py* script to create an alpha channel that can be used to exclude cloudy areas from visualization.

Ancillary\Mosaic_Map: The folder contains an ArcGIS 9.3 personal geodatabase containing the polygon files used to generate the mosaic. The polygon files were used to create the raster GRID files which were input into the mosaic scripts. The **top_pathid** GRID includes the acquisition date for each pixel used in the final mosaic. Other metadata fields may be linked via the path_id column using the data in Appendix 3.

Ancillary\Sample_Points: Contains sample locations, sample values, and supporting data used for the image to image radiometric calibration and the topographic normalization.

Ancillary\Study_Area: An ArcGIS 9.3 personal geodatabase containing the park boundaries, selected other federal lands, the study area bounding box, and the results of the WRS2 path coverage analysis.

DEM\GDEM: ASTER G-DEM elevation model and hillshade rasters for the study area.

DEM\NED: NED elevation model, hillshade, slope and aspect rasters for the study area.

DEM\raw: The original, unprojected data for the ASTER G-DEM and NED elevation models. The data have been mosaicked and clipped to the study area, but have not been resampled or tranformed.

eMODIS: Stacked eMODIS Alaska data (Jenkerson 2009) for 11 one-week composite periods, 25 June–9 September 2002. Includes both original 16-bit format, and calibrated 8-bit versions for faster display performance. In ArcGIS, use default two standard deviation stretch or minimum/maximum stretch to view 16-bit imagery with intended contrast calibration; use no stretch to view 8-bit imagery.

Landsat\01_browse\01a_usgs_jpg: Georeferenced Landsat browse images over the full ARCN study area, organized by path and row, through fall 2009. Each image has MM-DD-YYYY prepended to the name so that it can easily be sorted by day of year.

Landsat\01_browse\01b_fullres_jp2: Full resolution, contrast calibrated browse images for all scenes in the ABR inventory within the ARCN full study area, organized by path and row. The contrast calibration is accomplished by specially constructed aux.xml header files. In ArcGIS, use the default two standard deviation stretch or minimum/maximum stretch to view contrast calibration as intended. If present, the seventh band contains a rough cloud mask that may be loaded as an alpha channel.

Landsat\02_raw: Raw data files for all scenes in the ABR inventory over the full ARCN study area. Also includes LEDAPS algorithm outputs for selected scenes. Organized by path and row with one folder for each scene. See 02Raw_ReadMe.txt for file and folder naming conventions.

Landsat\03_top_of_atm_refl: Landsat swaths, calibrated to top-of-atmosphere reflectance following Chander 2009 parameters. Includes both original 16-bit format, and calibrated 8-bit versions for faster display performance. In ArcGIS, use default two standard deviation stretch or minimum/maximum stretch to view 16-bit imagery with intended contrast calibration; use no stretch to view 8-bit imagery.

Landsat\04_calibrated_top_of_atm_refl: Landsat swaths, calibrated by image-to-image calibration method to 29 July 2002 Landsat ETM+ top-of-atmosphere reflectance swath. Includes both original 16-bit format, and calibrated 8-bit versions for faster display performance. In ArcGIS, use default two

standard deviation stretch or minimum/maximum stretch to view 16-bit imagery with intended contrast calibration; use no stretch to view 8-bit imagery.

Landsat\05_surface_reflectance: Landsat swaths, calibrated to surface reflectance using LEDAPS algorithm (Masek 2006). Includes both original 16-bit format, and calibrated 8-bit versions for faster display performance. In ArcGIS, use default two standard deviation stretch or minimum/maximum stretch to view 16-bit imagery with intended contrast calibration; use no stretch to view 8-bit imagery.

Landsat\06_mosaic: Landsat mosaics for ARCN study area. Includes 1999, 2002, and alternate mosaics, each with partial coverage. Also includes merged mosaic with full coverage, constructed by merging mosaics from all three eras. Includes both original 16-bit format, and calibrated 8-bit versions for faster display performance. In ArcGIS, use default two standard deviation stretch or minimum/maximum stretch to view 16-bit imagery with intended contrast calibration; use no stretch to view 8-bit imagery.

Landsat\07_topo_norm_mosaic: Topographically normalized version of ARCN mosaic (full coverage version). Includes both original 16-bit format, and calibrated 8-bit versions for faster display performance. In ArcGIS, use default two standard deviation stretch or minimum/maximum stretch to view 16-bit imagery with intended contrast calibration; use no stretch to view 8-bit imagery.

Metadata: Templates used to generate and apply metadata to GIS data deliverables.

Report: PDF version of this report.

Scripts: Scripts used to search and preprocess Landsat imagery, and to produce the final swath and mosaic data products. Described in detail in Appendix 2.

WELD: Circa 2008 Landsat mosaic produced from the Web-Enabled Landsat Data project, version 1.5 (Roy 2010).

Appendix 2: Scripts

Scripts\01_browse\make_world_file.py: Python script that reads the metadata for each browse image and constructs an ArcGIS-compatible world file.

Scripts\01_browse\make_mm_dd_yyyy.py: Python script that renames browse images by prepending the text "MM-DD-YYYY_" to the filename of each browse image and world file, where MM is the two digit month, DD is the two digit day of month, and YYYY is the four digit year.

Scripts\02_raw\new_landsat_processing\new_landsat_processing.py: Python script that parses the output from the Landsat bulk download web page, and automatically downloads the packaged file for each image. It then unpacks the data, reads the associated metadata file and writes the metadata to a PostgreSQL database table. Finally, the script generates a full resolution, six band, contrast calibrated browse images in JPEG 2000 format from each downloaded image.

Scripts\03_top_of_atm_refl\landsat_jp2_toarefl.py: Python script that calculates top of atmosphere reflectance for each scene. The Python script converts the JPEG 2000 full resolution browse to 16-bit signed-integer format GeoTIFF images using the conversion factors stored in the metadata tables. Reflectance values were scaled by a factor of 10,000.

Scripts\04_calibrated_top_of_atm_refl.mdl files:* Erdas Imagine 2010 SML models that apply the slope and offset parameters necessary to convert the original top-of-atmosphere image to a calibrated image.

Scripts\05_surface_reflectance\ledaps: The Landsat Ecosystem Disturbance Adaptive Processing System (LEDAPS, http://ledaps.nascom.nasa.gov, Masek 2006). LEDAPS is provided as a set of C programs that run in a Unix or Linux environment. The LEDAPS subroutines calculate top of atmosphere reflectance, a cloud mask, aerosol optical depth and surface reflectance.

Scripts\05_surface_reflectance\ledaps\ledaps_wrapper.sh: A Bourne shell script that calls several C subroutines from the LEDAPS package.

Scripts\05_surface_reflectance\lndsr_hdf_to_tif.sh: A Bourne shell script that calls GDAL tools to convert the LEDAPS surface reflectance raster from HDF to GeoTiff format.

Scripts\05_surface_reflectance\reband_landsat_solar.py: Python script that appends a solar zenith angle band and solar azimuth angle band to the LEDAPS surface reflectance raster in GeoTIFF format. It also separates the LEDAPS QA/QC band into a separate raster. The fill value for the QA/QC band was different from that of the other bands and it was not properly processed by the subsequent swath mosaicking script.

Scripts\06_mosaic.gmd files*: Erdas Imagine 2010 graphical models that produce a mosaic from a set of Landsat swaths and a grid indicating the source imagery for each pixel in the mosaic.

Scripts\07_topo_norm_mosaic\cosi_cose_20100526.gmd: Erdas model file to calculate cosine of the slope and cosine of the solar incidence angle for the mosaic study area.

Scripts\07_topo_norm_mosaic\sample2sqlite.py: Python script that converts a text file to SQLite 3 format, which provides better performance and simpler programming for extracting subsets of data in the following script.

Scripts\07_topo_norm_mosaic\illum_regression.py: Python script that estimates k-values for various subsets of the sample data, running 10 trials for each subset.

Scripts\07_topo_norm_mosaic\illum_corr_20100611.gmd: Erdas model to combine k-images, terrain slope, solar incidence angle and surface reflectance to produce correction factors and topographically normalized mosaic.

Scripts\arcn_swath_mosaic_clip.py: Python script that mosaics the data from a single Landsat overpass comprising multiple rows. These data have the same WRS2 row and the same acquisition date. The script also clips the resulting mosaic to the bounding box of the full study area.

Scripts\convert_16bit_to_8bit_tif.mdl and *.bcf*: Erdas Imagine 2010 Spatial Modeler Language (SML) scripts and associated batch command files that automate the conversion of imagery in signed 16-bit format (generally with a scale factor of 10,000) to an unsigned 8-bit GeoTIFF image. A fixed contrast stretch is applied when generating the 8-bit image. The creation of 8-bit images is mainly a work-around for performance issues associated with displaying 16-bit signed integer format images in ArcGIS 9.3. The contrast stretch should be set to "None" when viewing the resulting 8-bit images in ArcGIS, Erdas Imagine, or other image viewing applications.

*Scripts\metadata\metadata.sh and *.sh:* A Bourne shell script that copies a prepared metadata file to an existing image, and updates the source date in the metadata to the specified value. Used in conjunction with the NPS Metadata Tools v. 1.1 to provide compliant metadata for the many GIS files included in data deliverable.

Project Raster (ArcToolbox 9.3.1): The batch mode of ArcGIS was used to reproject the individual Landsat scenes to the Alaska Albers (NAD1983) coordinate system. The ArcGIS tool includes the option to specify a snap raster in the output images.

Appendix 3. Landsat scenes considered for mosaic with selected metadata values.

Granule ID	PathID	Acquisition Date	WRS2 Path	WRS2 Row	Solar Azimuth	Solar Elevation	Product Type	Satellite	Sensor	d	$LMIN_1$	$LMAX_1$	$ESUN_1$	$LMIN_2$	$LMAX_2$	$ESUN_2$	$LMIN_3$	$LMAX_3$	$ESUN_3$	$LMIN_4$	$LMAX_4$	$ESUN_4$	$LMIN_5$	$LMAX_5$	$ESUN_5$	$LMIN_7$	$LMAX_7$	$ESUN_7$
LE70710132001174AGS00	713	2001-06-23	71	13	166.01	45.97	L1T	7	ETM+	1.0164	-6.20	191.60	1997.00	-6.40	196.50	1812.00	-5.00	152.90	1533.00	-5.10	241.10	1039.00	-1.00	31.06	230.80	-0.35	10.80	84.90
LE70710142001174AGS00	713	2001-06-23	71	14	163.97	47.15	L1T	7	ETM+	1.0164	-6.20	191.60	1997.00	-6.40	196.50	1812.00	-5.00	152.90	1533.00	-5.10	241.10	1039.00	-1.00	31.06	230.80	-0.35	10.80	84.90
LE70710152001174AGS00	713	2001-06-23	71	15	162.00	48.31	L1T	7	ETM+	1.0164	-6.20	293.70	1997.00	-6.40	300.90	1812.00	-5.00	234.40	1533.00	-5.10	241.10	1039.00	-1.00	31.06	230.80	-0.35	10.80	84.90
LE70720122002200PFS00	721	2002-07-19	72	12	166.81	42.02	L1T	7	ETM+	1.0162	-6.20	191.60	1997.00	-6.40	196.50	1812.00	-5.00	152.90	1533.00	-5.10	241.10	1039.00	-1.00	31.06	230.80	-0.35	10.80	84.90
LE70720122002216AGS00	722	2002-08-04	72	12	167.27	38.39	L1T	7	ETM+	1.0146	-6.20	191.60	1997.00	-6.40	196.50	1812.00	-5.00	152.90	1533.00	-5.10	241.10	1039.00	-1.00	31.06	230.80	-0.35	10.80	84.90
LE70720131999208AGS00	724	1999-07-27	72	13	166.47	41.72	L1T	7	ETM+	1.0155	-6.20	191.60	1997.00	-6.40	196.50	1812.00	-5.00	152.90	1533.00	-5.10	157.40	1039.00	-1.00	31.06	230.80	-0.35	10.80	84.90
LE70720132002200PFS00	721	2002-07-19	72	13	164.73	43.19	L1T	7	ETM+	1.0162	-6.20	191.60	1997.00	-6.40	196.50	1812.00	-5.00	152.90	1533.00	-5.10	241.10	1039.00	-1.00	31.06	230.80	-0.35	10.80	84.90
LE70720132002216AGS00	722	2002-08-04	72	13	165.29	39.57	L1T	7	ETM+	1.0146	-6.20	191.60	1997.00	-6.40	196.50	1812.00	-5.00	152.90	1533.00	-5.10	241.10	1039.00	-1.00	31.06	230.80	-0.35	10.80	84.90
LE70720141999208AGS00	724	1999-07-27	72	14	164.55	42.91	L1T	7	ETM+	1.0155	-6.20	191.60	1997.00	-6.40	196.50	1812.00	-5.00	152.90	1533.00	-5.10	157.40	1039.00	-1.00	31.06	230.80	-0.35	10.80	84.90
LE70720142002200PFS00	721	2002-07-19	72	14	162.74	44.35	L1T	7	ETM+	1.0162	-6.20	191.60	1997.00	-6.40	196.50	1812.00	-5.00	152.90	1533.00	-5.10	241.10	1039.00	-1.00	31.06	230.80	-0.35	10.80	84.90
LE70720142002216AGS00	722	2002-08-04	72	14	163.41	40.73	L1T	7	ETM+	1.0146	-6.20	191.60	1997.00	-6.40	196.50	1812.00	-5.00	152.90	1533.00	-5.10	241.10	1039.00	-1.00	31.06	230.80	-0.35	10.80	84.90
LE70720152002216AGS00	722	2002-08-04	72	15	161.61	41.89	L1T	7	ETM+	1.0146	-6.20	191.60	1997.00	-6.40	196.50	1812.00	-5.00	152.90	1533.00	-5.10	241.10	1039.00	-1.00	31.06	230.80	-0.35	10.80	84.90
LE70730111999183AGS00	733	1999-07-02	73	11	171.09	43.22	L1T	7	ETM+	1.0167	-6.20	191.60	1997.00	-6.40	196.50	1812.00	-5.00	152.90	1533.00	-5.10	157.40	1039.00	-1.00	31.06	230.80	-0.35	10.80	84.90
LE70730111999215AGS00	732	1999-08-03	73	11	170.89	37.62	L1T	7	ETM+	1.0147	-6.20	191.60	1997.00	-6.40	196.50	1812.00	-5.00	152.90	1533.00	-5.10	157.40	1039.00	-1.00	31.06	230.80	-0.35	10.80	84.90
LE70730112002191PFS00	734	2002-07-10	73	11	169.20	42.28	L1T	7	ETM+	1.0166	-6.20	191.60	1997.00	-6.40	196.50	1812.00	-5.00	152.90	1533.00	-5.10	241.10	1039.00	-1.00	31.06	230.80	-0.35	10.80	84.90
LE70730121999183AGS00	733	1999-07-02	73	12	168.85	44.42	L1T	7	ETM+	1.0167	-6.20	191.60	1997.00	-6.40	196.50	1812.00	-5.00	152.90	1533.00	-5.10	157.40	1039.00	-1.00	31.06	230.80	-0.35	10.80	84.90
LE70730121999215AGS00	732	1999-08-03	73	12	168.77	38.83	L1T	7	ETM+	1.0147	-6.20	191.60	1997.00	-6.40	196.50	1812.00	-5.00	152.90	1533.00	-5.10	157.40	1039.00	-1.00	31.06	230.80	-0.35	10.80	84.90
LE70730122002191PFS00	734	2002-07-10	73	12	166.95	43.46	L1T	7	ETM+	1.0166	-6.20	191.60	1997.00	-6.40	196.50	1812.00	-5.00	152.90	1533.00	-5.10	241.10	1039.00	-1.00	31.06	230.80	-0.35	10.80	84.90
LE70730131999183AGS00	733	1999-07-02	73	13	166.72	45.62	L1T	7	ETM+	1.0167	-6.20	191.60	1997.00	-6.40	196.50	1812.00	-5.00	152.90	1533.00	-5.10	157.40	1039.00	-1.00	31.06	230.80	-0.35	10.80	84.90
LE70730131999215AGS00	732	1999-08-03	73	13	166.80	40.02	L1T	7	ETM+	1.0147	-6.20	191.60	1997.00	-6.40	196.50	1812.00	-5.00	152.90	1533.00	-5.10	157.40	1039.00	-1.00	31.06	230.80	-0.35	10.80	84.90
LE70730132002191PFS00	734	2002-07-10	73	13	164.83	44.63	L1T	7	ETM+	1.0166	-6.20	191.60	1997.00	-6.40	196.50	1812.00	-5.00	152.90	1533.00	-5.10	241.10	1039.00	-1.00	31.06	230.80	-0.35	10.80	84.90
LE70730141999183AGS00	733	1999-07-02	73	14	164.70	46.80	L1T	7	ETM+	1.0167	-6.20	191.60	1997.00	-6.40	196.50	1812.00	-5.00	152.90	1533.00	-5.10	157.40	1039.00	-1.00	31.06	230.80	-0.35	10.80	84.90
LE70730141999215AGS00	732	1999-08-03	73	14	164.93	41.21	L1T	7	ETM+	1.0147	-6.20	191.60	1997.00	-6.40	196.50	1812.00	-5.00	152.90	1533.00	-5.10	157.40	1039.00	-1.00	31.06	230.80	-0.35	10.80	84.90
LE70730142002191PFS00	734	2002-07-10	73	14	162.80	45.78	L1T	7	ETM+	1.0166	-6.20	191.60	1997.00	-6.40	196.50	1812.00	-5.00	152.90	1533.00	-5.10	241.10	1039.00	-1.00	31.06	230.80	-0.35	10.80	84.90
LE70740112002214PFS00	741	2002-08-02	74	11	169.30	37.73	L1T	7	ETM+	1.0148	-6.20	191.60	1997.00	-6.40	196.50	1812.00	-5.00	152.90	1533.00	-5.10	241.10	1039.00	-1.00	31.06	230.80	-0.35	10.80	84.90
LE70740122002214PFS00	741	2002-08-02	74	12	167.17	38.91	L1T	7	ETM+	1.0148	-6.20	191.60	1997.00	-6.40	196.50	1812.00	-5.00	152.90	1533.00	-5.10	241.10	1039.00	-1.00	31.06	230.80	-0.35	10.80	84.90
LE70740122002230AGS01	743	2002-08-18	74	12	168.33	34.28	L1T	7	ETM+	1.0122	-6.20	191.60	1997.00	-6.40	196.50	1812.00	-5.00	152.90	1533.00	-5.10	157.40	1039.00	-1.00	31.06	230.80	-0.35	10.80	84.90
LE70740132002214PFS00	741	2002-08-02	74	13	165.17	40.09	L1T	7	ETM+	1.0148	-6.20	191.60	1997.00	-6.40	196.50	1812.00	-5.00	152.90	1533.00	-5.10	241.10	1039.00	-1.00	31.06	230.80	-0.35	10.80	84.90
LE70740142002214PFS00	741	2002-08-02	74	14	163.27	41.25	L1T	7	ETM+	1.0148	-6.20	191.60	1997.00	-6.40	196.50	1812.00	-5.00	152.90	1533.00	-5.10	241.10	1039.00	-1.00	31.06	230.80	-0.35	10.80	84.90
LE70740152002214PFS00	741	2002-08-02	74	15	161.46	42.40	L1T	7	ETM+	1.0148	-6.20	191.60	1997.00	-6.40	196.50	1812.00	-5.00	152.90	1533.00	-5.10	241.10	1039.00	-1.00	31.06	230.80	-0.35	10.80	84.90
LE70750111999181AGS00	752	1999-06-30	75	11	171.20	43.36	L1T	7	ETM+	1.0166	-6.20	191.60	1997.00	-6.40	196.50	1812.00	-5.00	152.90	1533.00	-5.10	157.40	1039.00	-1.00	31.06	230.80	-0.35	10.80	84.90
LE70750112002205PFS00	751	2002-07-24	75	11	169.04	39.85	L1T	7	ETM+	1.0158	-6.20	191.60	1997.00	-6.40	196.50	1812.00	-5.00	152.90	1533.00	-5.10	241.10	1039.00	-1.00	31.06	230.80	-0.35	10.80	84.90
LE70750121999181AGS00	752	1999-06-30	75	12	168.95	44.57	L1T	7	ETM+	1.0166	-6.20	191.60	1997.00	-6.40	196.50	1812.00	-5.00	152.90	1533.00	-5.10	157.40	1039.00	-1.00	31.06	230.80	-0.35	10.80	84.90
LE70750122002205PFS00	751	2002-07-24	75	12	166.86	41.03	L1T	7	ETM+	1.0158	-6.20	191.60	1997.00	-6.40	196.50	1812.00	-5.00	152.90	1533.00	-5.10	241.10	1039.00	-1.00	31.06	230.80	-0.35	10.80	84.90
LE70750131999181AGS00	752	1999-06-30	75	13	166.83	45.76	L1T	7	ETM+	1.0166	-6.20	191.60	1997.00	-6.40	196.50	1812.00	-5.00	152.90	1533.00	-5.10	157.40	1039.00	-1.00	31.06	230.80	-0.35	10.80	84.90
LE70750132002205PFS00	751	2002-07-24	75	13	164.80	42.20	L1T	7	ETM+	1.0158	-6.20	191.60	1997.00	-6.40	196.50	1812.00	-5.00	152.90	1533.00	-5.10	241.10	1039.00	-1.00	31.06	230.80	-0.35	10.80	84.90
LE70750141999181AGS00	752	1999-06-30	75	14	164.80	46.95	L1T	7	ETM+	1.0166	-6.20	191.60	1997.00	-6.40	196.50	1812.00	-5.00	152.90	1533.00	-5.10	157.40	1039.00	-1.00	31.06	230.80	-0.35	10.80	84.90
LE70750142002205PFS00	751	2002-07-24	75	14	162.85	43.35	L1T	7	ETM+	1.0158	-6.20	191.60	1997.00	-6.40	196.50	1812.00	-5.00	152.90	1533.00	-5.10	241.10	1039.00	-1.00	31.06	230.80	-0.35	10.80	84.90
LE70760112002212PFS00	761	2002-07-31	76	11	169.22	38.23	L1T	7	ETM+	1.0151	-6.20	293.70	1997.00	-6.40	300.90	1812.00	-5.00	234.40	1533.00	-5.10	241.10	1039.00	-1.00	31.06	230.80	-0.35	10.80	84.90
LE70760112003199EDC02	762	2003-07-18	76	11	169.09	41.07	L1T	7	ETM+	1.0163	-6.20	293.70	1997.00	-6.40	300.90	1812.00	-5.00	234.40	1533.00	-5.10	241.10	1039.00	-1.00	31.06	230.80	-0.35	10.80	84.90
LE70760122002212PFS00	761	2002-07-31	76	12	167.07	39.42	L1T	7	ETM+	1.0151	-6.20	191.60	1997.00	-6.40	196.50	1812.00	-5.00	152.90	1533.00	-5.10	241.10	1039.00	-1.00	31.06	230.80	-0.35	10.80	84.90
LE70760122003199EDC02	762	2003-07-18	76	12	166.87	42.25	L1T	7	ETM+	1.0163	-6.20	293.70	1997.00	-6.40	300.90	1812.00	-5.00	234.40	1533.00	-5.10	241.10	1039.00	-1.00	31.06	230.80	-0.35	10.80	84.90
LE70760132002212PFS00	761	2002-07-31	76	13	165.06	40.59	L1T	7	ETM+	1.0151	-6.20	191.60	1997.00	-6.40	196.50	1812.00	-5.00	152.90	1533.00	-5.10	241.10	1039.00	-1.00	31.06	230.80	-0.35	10.80	84.90
LE70760142002212PFS00	761	2002-07-31	76	14	163.15	41.75	L1T	7	ETM+	1.0151	-6.20	191.60	1997.00	-6.40	196.50	1812.00	-5.00	152.90	1533.00	-5.10	241.10	1039.00	-1.00	31.06	230.80	-0.35	10.80	84.90
LE70760142003199EDC02	762	2003-07-18	76	14	162.78	44.58	L1T	7	ETM+	1.0163	-6.20	293.70	1997.00	-6.40	300.90	1812.00	-5.00	234.40	1533.00	-5.10	241.10	1039.00	-1.00	31.06	230.80	-0.35	10.80	84.90
LE70760152002212PFS00	761	2002-07-31	76	15	161.33	42.90	L1T	7	ETM+	1.0151	-6.20	191.60	1997.00	-6.40	196.50	1812.00	-5.00	152.90	1533.00	-5.10	241.10	1039.00	-1.00	31.06	230.80	-0.35	10.80	84.90
LE70770122002219PFS00	771	2002-08-07	77	12	167.45	37.57	L1T	7	ETM+	1.0141	-6.20	191.60	1997.00	-6.40	196.50	1812.00	-5.00	152.90	1533.00	-5.10	157.40	1039.00	-1.00	31.06	230.80	-0.35	10.80	84.90
LE70770122005179EDC00	774	2005-06-28	77	12	167.75	44.59	L1T	7	ETM+	1.0166	-6.20	191.60	1997.00	-6.40	196.50	1812.00	-5.00	152.90	1533.00	-5.10	241.10	1039.00	-1.00	31.06	230.80	-0.35	10.80	84.90
LE70770132002219PFS00	771	2002-08-07	77	13	165.49	38.75	L1T	7	ETM+	1.0141	-6.20	191.60	1997.00	-6.40	196.50	1812.00	-5.00	152.90	1533.00	-5.10	157.40	1039.00	-1.00	31.06	230.80	-0.35	10.80	84.90
LE70770132005179EDC00	774	2005-06-28	77	13	165.61	45.77	L1T	7	ETM+	1.0166	-6.20	191.60	1997.00	-6.40	196.50	1812.00	-5.00	152.90	1533.00	-5.10	241.10	1039.00	-1.00	31.06	230.80	-0.35	10.80	84.90
LE70770142002219PFS00	771	2002-08-07	77	14	163.64	39.92	L1T	7	ETM+	1.0141	-6.20	191.60	1997.00	-6.40	196.50	1812.00	-5.00	152.90	1533.00	-5.10	157.40	1039.00	-1.00	31.06	230.80	-0.35	10.80	84.90
LE70780112002210PFS00	781	2002-07-29	78	11	169.16	38.72	L1T	7	ETM+	1.0153	-6.20	293.70	1997.00	-6.40	300.90	1812.00	-5.00	234.40	1533.00	-5.10	241.10	1039.00	-1.00	31.06	230.80	-0.35	10.80	84.90
LE70780122002210PFS00	781	2002-07-29	78	12	166.99	39.90	L1T	7	ETM+	1.0153	-6.20	293.70	1997.00	-6.40	300.90	1812.00	-5.00	234.40	1533.00	-5.10	241.10	1039.00	-1.00	31.06	230.80	-0.35	10.80	84.90
LE70780132002210PFS00	781	2002-07-29	78	13	164.97	41.07	L1T	7	ETM+	1.0153	-6.20	293.70	1997.00	-6.40	300.90	1812.00	-5.00	234.40	1533.00	-5.10	241.10	1039.00	-1.00	31.06	230.80	-0.35	10.80	84.90

Appendix 3. Landsat scenes considered for mosaic with selected metadata values.

Granule ID	PathID	Acquisition Date	WRS2 Path	WRS2 Row	Solar Azimuth	Solar Elevation	Product Type	Satellite	Sensor	d	$LMIN_1$	$LMAX_1$	$ESUN_1$	$LMIN_2$	$LMAX_2$	$ESUN_2$	$LMIN_3$	$LMAX_3$	$ESUN_3$	$LMIN_4$	$LMAX_4$	$ESUN_4$	$LMIN_5$	$LMAX_5$	$ESUN_5$	$LMIN_7$	$LMAX_7$	$ESUN_7$
LE70780142002210PFS00	781	2002-07-29	78	14	163.05	42.23	L1T	7	ETM+	1.0153	-6.20	293.70	1997.00	-6.40	300.90	1812.00	-5.00	234.40	1533.00	-5.10	241.10	1039.00	-1.00	31.06	230.80	-0.35	10.80	84.90
LE70790111999209AGS00	793	1999-07-28	79	11	170.68	39.09	L1T	7	ETM+	1.0154	-6.20	191.60	1997.00	-6.40	196.50	1812.00	-5.00	152.90	1533.00	-5.10	157.40	1039.00	-1.00	31.06	230.80	-0.35	10.80	84.90
LE70790112002201AGS00	796	2002-07-20	79	11	169.03	40.65	L1T	7	ETM+	1.0162	-6.20	191.60	1997.00	-6.40	196.50	1812.00	-5.00	152.90	1533.00	-5.10	157.40	1039.00	-1.00	31.06	230.80	-0.35	10.80	84.90
LE70790121999209AGS00	793	1999-07-28	79	12	168.53	40.30	L1T	7	ETM+	1.0154	-6.20	191.60	1997.00	-6.40	196.50	1812.00	-5.00	152.90	1533.00	-5.10	157.40	1039.00	-1.00	31.06	230.80	-0.35	10.80	84.90
LE70790122000180AGS00	795	2000-06-28	79	12	168.53	44.62	L1T	7	ETM+	1.0166	-6.20	191.60	1997.00	-6.40	196.50	1812.00	-5.00	152.90	1533.00	-5.10	241.10	1039.00	-1.00	31.06	230.80	-0.35	10.80	84.90
LE70790122002201AGS00	796	2002-07-20	79	12	166.82	41.83	L1T	7	ETM+	1.0162	-6.20	191.60	1997.00	-6.40	196.50	1812.00	-5.00	152.90	1533.00	-5.10	157.40	1039.00	-1.00	31.06	230.80	-0.35	10.80	84.90
LE70790122002217PFS00	791	2002-08-05	79	12	167.33	38.12	L1T	7	ETM+	1.0144	-6.20	191.60	1997.00	-6.40	196.50	1812.00	-5.00	152.90	1533.00	-5.10	241.10	1039.00	-1.00	31.06	230.80	-0.35	10.80	84.90
LE70790122002233PFS00	792	2002-08-21	79	12	168.63	33.30	L1T	7	ETM+	1.0117	-6.20	191.60	1997.00	-6.40	196.50	1812.00	-5.00	152.90	1533.00	-5.10	157.40	1039.00	-1.00	31.06	230.80	-0.35	10.80	84.90
LE70790131999209AGS00	793	1999-07-28	79	13	166.51	41.49	L1T	7	ETM+	1.0154	-6.20	191.60	1997.00	-6.40	196.50	1812.00	-5.00	152.90	1533.00	-5.10	157.40	1039.00	-1.00	31.06	230.80	-0.35	10.80	84.90
LE70790132000180AGS00	795	2000-06-28	79	13	166.40	45.81	L1T	7	ETM+	1.0166	-6.20	191.60	1997.00	-6.40	196.50	1812.00	-5.00	152.90	1533.00	-5.10	241.10	1039.00	-1.00	31.06	230.80	-0.35	10.80	84.90
LE70790132002201AGS00	796	2002-07-20	79	13	164.74	43.00	L1T	7	ETM+	1.0162	-6.20	191.60	1997.00	-6.40	196.50	1812.00	-5.00	152.90	1533.00	-5.10	241.10	1039.00	-1.00	31.06	230.80	-0.35	10.80	84.90
LE70790132002217PFS00	791	2002-08-05	79	13	165.35	39.29	L1T	7	ETM+	1.0144	-6.20	191.60	1997.00	-6.40	196.50	1812.00	-5.00	152.90	1533.00	-5.10	241.10	1039.00	-1.00	31.06	230.80	-0.35	10.80	84.90
LE70790132002233PFS00	792	2002-08-21	79	13	166.78	34.49	L1T	7	ETM+	1.0117	-6.20	191.60	1997.00	-6.40	196.50	1812.00	-5.00	152.90	1533.00	-5.10	157.40	1039.00	-1.00	31.06	230.80	-0.35	10.80	84.90
LE70790142000180AGS00	795	2000-06-28	79	14	164.37	46.99	L1T	7	ETM+	1.0166	-6.20	191.60	1997.00	-6.40	196.50	1812.00	-5.00	152.90	1533.00	-5.10	241.10	1039.00	-1.00	31.06	230.80	-0.35	10.80	84.90
LE70790142002201AGS00	796	2002-07-20	79	14	162.76	44.16	L1T	7	ETM+	1.0162	-6.20	191.60	1997.00	-6.40	196.50	1812.00	-5.00	152.90	1533.00	-5.10	241.10	1039.00	-1.00	31.06	230.80	-0.35	10.80	84.90
LE70790142002233PFS00	792	2002-08-21	79	14	165.04	35.68	L1T	7	ETM+	1.0117	-6.20	191.60	1997.00	-6.40	196.50	1812.00	-5.00	152.90	1533.00	-5.10	157.40	1039.00	-1.00	31.06	230.80	-0.35	10.80	84.90
LE70790152000180AGS00	795	2000-06-28	79	15	162.41	48.16	L1T	7	ETM+	1.0166	-6.20	191.60	1997.00	-6.40	196.50	1812.00	-5.00	152.90	1533.00	-5.10	241.10	1039.00	-1.00	31.06	230.80	-0.35	10.80	84.90
LE70800112002208AGS00	801	2002-07-27	80	11	169.10	39.18	L1T	7	ETM+	1.0155	-6.20	293.70	1997.00	-6.40	300.90	1812.00	-5.00	234.40	1533.00	-5.10	241.10	1039.00	-1.00	31.06	230.80	-0.35	10.80	84.90
LE70800122002192AGS00	803	2002-07-11	80	12	166.92	43.32	L1T	7	ETM+	1.0166	-6.20	293.70	1997.00	-6.40	300.90	1812.00	-5.00	234.40	1533.00	-5.10	241.10	1039.00	-1.00	31.06	230.80	-0.35	10.80	84.90
LE70800122002208AGS00	801	2002-07-27	80	12	166.93	40.36	L1T	7	ETM+	1.0155	-6.20	293.70	1997.00	-6.40	300.90	1812.00	-5.00	234.40	1533.00	-5.10	241.10	1039.00	-1.00	31.06	230.80	-0.35	10.80	84.90
LE70800122002224PFS00	804	2002-08-12	80	12	167.81	36.12	L1T	7	ETM+	1.0133	-6.20	293.70	1997.00	-6.40	300.90	1812.00	-5.00	234.40	1533.00	-5.10	241.10	1039.00	-1.00	31.06	230.80	-0.35	10.80	84.90
LE70800132002192AGS00	803	2002-07-11	80	13	164.79	44.49	L1T	7	ETM+	1.0166	-6.20	293.70	1997.00	-6.40	300.90	1812.00	-5.00	234.40	1533.00	-5.10	241.10	1039.00	-1.00	31.06	230.80	-0.35	10.80	84.90
LE70800132002208AGS00	801	2002-07-27	80	13	164.89	41.53	L1T	7	ETM+	1.0155	-6.20	293.70	1997.00	-6.40	300.90	1812.00	-5.00	234.40	1533.00	-5.10	241.10	1039.00	-1.00	31.06	230.80	-0.35	10.80	84.90
LE70800132002224PFS00	804	2002-08-12	80	13	165.89	37.31	L1T	7	ETM+	1.0133	-6.20	293.70	1997.00	-6.40	300.90	1812.00	-5.00	234.40	1533.00	-5.10	241.10	1039.00	-1.00	31.06	230.80	-0.35	10.80	84.90
LE70800142002208AGS00	801	2002-07-27	80	14	162.96	42.69	L1T	7	ETM+	1.0155	-6.20	293.70	1997.00	-6.40	300.90	1812.00	-5.00	234.40	1533.00	-5.10	241.10	1039.00	-1.00	31.06	230.80	-0.35	10.80	84.90
LE70800142002224PFS00	804	2002-08-12	80	14	164.08	38.48	L1T	7	ETM+	1.0133	-6.20	293.70	1997.00	-6.40	300.90	1812.00	-5.00	234.40	1533.00	-5.10	241.10	1039.00	-1.00	31.06	230.80	-0.35	10.80	84.90
LE70800152002208AGS00	801	2002-07-27	80	15	161.10	43.84	L1T	7	ETM+	1.0155	-6.20	293.70	1997.00	-6.40	300.90	1812.00	-5.00	234.40	1533.00	-5.10	241.10	1039.00	-1.00	31.06	230.80	-0.35	10.80	84.90
LE70810112002199AGS00	812	2002-07-18	81	11	169.04	41.02	L1T	7	ETM+	1.0163	-6.20	293.70	1997.00	-6.40	300.90	1812.00	-5.00	234.40	1533.00	-5.10	241.10	1039.00	-1.00	31.06	230.80	-0.35	10.80	84.90
LE70810112002215AGS01	811	2002-08-03	81	11	169.35	37.46	L1T	7	ETM+	1.0147	-6.20	191.60	1997.00	-6.40	196.50	1812.00	-5.00	152.90	1533.00	-5.10	157.40	1039.00	-1.00	31.06	230.80	-0.35	10.80	84.90
LE70810122002199AGS00	812	2002-07-18	81	12	166.81	42.20	L1T	7	ETM+	1.0163	-6.20	293.70	1997.00	-6.40	300.90	1812.00	-5.00	234.40	1533.00	-5.10	241.10	1039.00	-1.00	31.06	230.80	-0.35	10.80	84.90
LE70810122002215AGS01	811	2002-08-03	81	12	167.22	38.65	L1T	7	ETM+	1.0147	-6.20	191.60	1997.00	-6.40	196.50	1812.00	-5.00	152.90	1533.00	-5.10	157.40	1039.00	-1.00	31.06	230.80	-0.35	10.80	84.90
LE70810132002199AGS00	812	2002-07-18	81	13	164.72	43.37	L1T	7	ETM+	1.0163	-6.20	293.70	1997.00	-6.40	300.90	1812.00	-5.00	234.40	1533.00	-5.10	241.10	1039.00	-1.00	31.06	230.80	-0.35	10.80	84.90
LE70810132002215AGS01	811	2002-08-03	81	13	165.23	39.82	L1T	7	ETM+	1.0147	-6.20	191.60	1997.00	-6.40	196.50	1812.00	-5.00	152.90	1533.00	-5.10	157.40	1039.00	-1.00	31.06	230.80	-0.35	10.80	84.90
LE70810142002199AGS00	812	2002-07-18	81	14	162.73	44.52	L1T	7	ETM+	1.0163	-6.20	293.70	1997.00	-6.40	300.90	1812.00	-5.00	234.40	1533.00	-5.10	241.10	1039.00	-1.00	31.06	230.80	-0.35	10.80	84.90
LE70810142002215AGS01	811	2002-08-03	81	14	163.34	40.99	L1T	7	ETM+	1.0147	-6.20	191.60	1997.00	-6.40	196.50	1812.00	-5.00	152.90	1533.00	-5.10	157.40	1039.00	-1.00	31.06	230.80	-0.35	10.80	84.90
LE70810152002199AGS00	812	2002-07-18	81	15	160.81	45.67	L1T	7	ETM+	1.0163	-6.20	293.70	1997.00	-6.40	300.90	1812.00	-5.00	234.40	1533.00	-5.10	241.10	1039.00	-1.00	31.06	230.80	-0.35	10.80	84.90
LE70810152002215AGS01	811	2002-08-03	81	15	161.54	42.14	L1T	7	ETM+	1.0147	-6.20	191.60	1997.00	-6.40	196.50	1812.00	-5.00	152.90	1533.00	-5.10	157.40	1039.00	-1.00	31.06	230.80	-0.35	10.80	84.90
LE70820122002206AGS00	821	2002-07-25	82	12	166.88	40.81	L1T	7	ETM+	1.0157	-6.20	293.70	1997.00	-6.40	300.90	1812.00	-5.00	234.40	1533.00	-5.10	241.10	1039.00	-1.00	31.06	230.80	-0.35	10.80	84.90
LE70820132002206AGS00	821	2002-07-25	82	13	164.83	41.98	L1T	7	ETM+	1.0157	-6.20	293.70	1997.00	-6.40	300.90	1812.00	-5.00	234.40	1533.00	-5.10	241.10	1039.00	-1.00	31.06	230.80	-0.35	10.80	84.90
LE70820142002206AGS00	821	2002-07-25	82	14	162.88	43.13	L1T	7	ETM+	1.0157	-6.20	293.70	1997.00	-6.40	300.90	1812.00	-5.00	234.40	1533.00	-5.10	241.10	1039.00	-1.00	31.06	230.80	-0.35	10.80	84.90
LE70830112002213AGS00	831	2002-08-01	83	11	169.26	37.98	L1T	7	ETM+	1.0150	-6.20	191.60	1997.00	-6.40	196.50	1812.00	-5.00	152.90	1533.00	-5.10	157.40	1039.00	-1.00	31.06	230.80	-0.35	10.80	84.90
LE70830122002213AGS00	831	2002-08-01	83	12	167.12	39.16	L1T	7	ETM+	1.0150	-6.20	191.60	1997.00	-6.40	196.50	1812.00	-5.00	152.90	1533.00	-5.10	157.40	1039.00	-1.00	31.06	230.80	-0.35	10.80	84.90
LE70830132002213AGS00	831	2002-08-01	83	13	165.11	40.33	L1T	7	ETM+	1.0150	-6.20	191.60	1997.00	-6.40	196.50	1812.00	-5.00	152.90	1533.00	-5.10	157.40	1039.00	-1.00	31.06	230.80	-0.35	10.80	84.90
LE70830142000192AGS01	832	2000-07-10	83	14	163.86	45.81	L1T	7	ETM+	1.0166	-6.20	191.60	1997.00	-6.40	196.50	1812.00	-5.00	152.90	1533.00	-5.10	241.10	1039.00	-1.00	31.06	230.80	-0.35	10.80	84.90
LE70830142002213AGS00	831	2002-08-01	83	14	163.21	41.49	L1T	7	ETM+	1.0150	-6.20	191.60	1997.00	-6.40	196.50	1812.00	-5.00	152.90	1533.00	-5.10	157.40	1039.00	-1.00	31.06	230.80	-0.35	10.80	84.90
LT40740111989210XXX02	742	1989-07-29	74	11	164.85	38.41	L1T	4	TM	1.0153	-1.52	171.00	1983.00	-2.84	336.00	1795.00	-1.17	254.00	1539.00	-1.51	221.00	1028.00	-0.37	31.40	219.80	-0.15	16.60	83.49
LT40740121989210XXX02	742	1989-07-29	74	12	162.61	39.53	L1T	4	TM	1.0153	-1.52	171.00	1983.00	-2.84	336.00	1795.00	-1.17	254.00	1539.00	-1.51	221.00	1028.00	-0.37	31.40	219.80	-0.15	16.60	83.49
LT50710131999177XXX02	711	1999-06-26	71	13	162.14	45.58	L1T	5	TM	1.0165	-1.52	193.00	1983.00	-2.84	365.00	1796.00	-1.17	264.00	1536.00	-1.51	221.00	1031.00	-0.37	30.20	220.00	-0.15	16.50	83.44
LT50710131999193XXX02	714	1999-07-12	71	13	161.45	44.08	L1T	5	TM	1.0166	-1.52	193.00	1983.00	-2.84	365.00	1796.00	-1.17	264.00	1536.00	-1.51	221.00	1031.00	-0.37	30.20	220.00	-0.15	16.50	83.44
LT50710141999177XXX02	711	1999-06-26	71	14	160.00	46.70	L1T	5	TM	1.0165	-1.52	193.00	1983.00	-2.84	365.00	1796.00	-1.17	264.00	1536.00	-1.51	221.00	1031.00	-0.37	30.20	220.00	-0.15	16.50	83.44
LT50710141999193XXX02	714	1999-07-12	71	14	159.35	45.19	L1T	5	TM	1.0166	-1.52	193.00	1983.00	-2.84	365.00	1796.00	-1.17	264.00	1536.00	-1.51	221.00	1031.00	-0.37	30.20	220.00	-0.15	16.50	83.44
LT50710151999177XXX02	711	1999-06-26	71	15	157.97	47.79	L1T	5	TM	1.0165	-1.52	193.00	1983.00	-2.84	365.00	1796.00	-1.17	264.00	1536.00	-1.51	221.00	1031.00	-0.37	30.20	220.00	-0.15	16.50	83.44
LT50720121999184AAA02	723	1999-07-03	72	12	163.92	44.01	L1T	5	TM	1.0167	-1.52	193.00	1983.00	-2.84	365.00	1796.00	-1.17	264.00	1536.00	-1.51	221.00	1031.00	-0.37	30.20	220.00	-0.15	16.50	83.44
LT50720131999184AAA02	723	1999-07-03	72	13	161.74	45.12	L1T	5	TM	1.0167	-1.52	193.00	1983.00	-2.84	365.00	1796.00	-1.17	264.00	1536.00	-1.51	221.00	1031.00	-0.37	30.20	220.00	-0.15	16.50	83.44

Appendix 3. Landsat scenes considered for mosaic with selected metadata values.

Granule ID	PathID	Acquisition Date	WRS2 Path	WRS2 Row	Solar Azimuth	Solar Elevation	Product Type	Satellite	Sensor	d	$LMIN_1$	$LMAX_1$	$ESUN_1$	$LMIN_2$	$LMAX_2$	$ESUN_2$	$LMIN_3$	$LMAX_3$	$ESUN_3$	$LMIN_4$	$LMAX_4$	$ESUN_4$	$LMIN_5$	$LMAX_5$	$ESUN_5$	$LMIN_7$	$LMAX_7$	$ESUN_7$
LT50770122005203GLC00	772	2005-07-22	77	12	166.83	41.39	L1T	5	TM	1.0160	-1.52	193.00	1983.00	-2.84	365.00	1796.00	-1.17	264.00	1536.00	-1.51	221.00	1031.00	-0.37	30.20	220.00	-0.15	16.50	83.44
LT50770122008180GLC00	773	2008-06-28	77	12	167.08	44.51	L1T	5	TM	1.0166	-1.52	193.00	1983.00	-2.84	365.00	1796.00	-1.17	264.00	1536.00	-1.51	221.00	1031.00	-0.37	30.20	220.00	-0.15	16.50	83.44
LT50770132005203GLC00	772	2005-07-22	77	13	164.76	42.54	L1T	5	TM	1.0160	-1.52	193.00	1983.00	-2.84	365.00	1796.00	-1.17	264.00	1536.00	-1.51	221.00	1031.00	-0.37	30.20	220.00	-0.15	16.50	83.44
LT50770132008180GLC00	773	2008-06-28	77	13	164.94	45.67	L1T	5	TM	1.0166	-1.52	193.00	1983.00	-2.84	365.00	1796.00	-1.17	264.00	1536.00	-1.51	221.00	1031.00	-0.37	30.20	220.00	-0.15	16.50	83.44
LT50770142005203GLC00	772	2005-07-22	77	14	162.77	43.71	L1T	5	TM	1.0160	-1.52	193.00	1983.00	-2.84	365.00	1796.00	-1.17	264.00	1536.00	-1.51	221.00	1031.00	-0.37	30.20	220.00	-0.15	16.50	83.44
LT50770142008180GLC00	773	2008-06-28	77	14	162.87	46.84	L1T	5	TM	1.0166	-1.52	193.00	1983.00	-2.84	365.00	1796.00	-1.17	264.00	1536.00	-1.51	221.00	1031.00	-0.37	30.20	220.00	-0.15	16.50	83.44
LT50770152005203GLC00	772	2005-07-22	77	15	160.89	44.85	L1T	5	TM	1.0160	-1.52	193.00	1983.00	-2.84	365.00	1796.00	-1.17	264.00	1536.00	-1.51	221.00	1031.00	-0.37	30.20	220.00	-0.15	16.50	83.44
LT50770152008180GLC00	773	2008-06-28	77	15	160.89	47.98	L1T	5	TM	1.0166	-1.52	193.00	1983.00	-2.84	365.00	1796.00	-1.17	264.00	1536.00	-1.51	221.00	1031.00	-0.37	30.20	220.00	-0.15	16.50	83.44
LT50780112008187GLC00	782	2008-07-05	78	11	168.93	42.75	L1T	5	TM	1.0167	-1.52	193.00	1983.00	-2.84	365.00	1796.00	-1.17	264.00	1536.00	-1.51	221.00	1031.00	-0.37	30.20	220.00	-0.15	16.50	83.44
LT50780122008187GLC00	782	2008-07-05	78	12	166.67	43.93	L1T	5	TM	1.0167	-1.52	193.00	1983.00	-2.84	365.00	1796.00	-1.17	264.00	1536.00	-1.51	221.00	1031.00	-0.37	30.20	220.00	-0.15	16.50	83.44
LT50780132008187GLC00	782	2008-07-05	78	13	164.53	45.09	L1T	5	TM	1.0167	-1.52	193.00	1983.00	-2.84	365.00	1796.00	-1.17	264.00	1536.00	-1.51	221.00	1031.00	-0.37	30.20	220.00	-0.15	16.50	83.44
LT50780142007184MGR00	783	2007-07-03	78	14	164.94	46.74	L1T	5	TM	1.0167	-1.52	193.00	1983.00	-2.84	365.00	1796.00	-1.17	264.00	1536.00	-1.51	221.00	1031.00	-0.37	30.20	220.00	-0.15	16.50	83.44
LT50780142008187GLC00	782	2008-07-05	78	14	162.47	46.25	L1T	5	TM	1.0167	-1.52	193.00	1983.00	-2.84	365.00	1796.00	-1.17	264.00	1536.00	-1.51	221.00	1031.00	-0.37	30.20	220.00	-0.15	16.50	83.44
LT50780152007184MGR00	783	2007-07-03	78	15	163.01	47.91	L1T	5	TM	1.0167	-1.52	193.00	1983.00	-2.84	365.00	1796.00	-1.17	264.00	1536.00	-1.51	221.00	1031.00	-0.37	30.20	220.00	-0.15	16.50	83.44
LT50780152008187GLC00	782	2008-07-05	78	15	160.51	47.39	L1T	5	TM	1.0167	-1.52	193.00	1983.00	-2.84	365.00	1796.00	-1.17	264.00	1536.00	-1.51	221.00	1031.00	-0.37	30.20	220.00	-0.15	16.50	83.44
LT50790132008210GLC00	794	2008-07-28	79	13	164.38	41.10	L1T	5	TM	1.0153	-1.52	193.00	1983.00	-2.84	365.00	1796.00	-1.17	264.00	1536.00	-1.51	221.00	1031.00	-0.37	30.20	220.00	-0.15	16.50	83.44
LT50790142008210GLC00	794	2008-07-28	79	14	162.42	42.27	L1T	5	TM	1.0153	-1.52	193.00	1983.00	-2.84	365.00	1796.00	-1.17	264.00	1536.00	-1.51	221.00	1031.00	-0.37	30.20	220.00	-0.15	16.50	83.44
LT50800122008185GLC00	802	2008-07-03	80	12	166.77	44.13	L1T	5	TM	1.0167	-1.52	193.00	1983.00	-2.84	365.00	1796.00	-1.17	264.00	1536.00	-1.51	221.00	1031.00	-0.37	30.20	220.00	-0.15	16.50	83.44
LT50800132008185GLC00	802	2008-07-03	80	13	164.63	45.29	L1T	5	TM	1.0167	-1.52	193.00	1983.00	-2.84	365.00	1796.00	-1.17	264.00	1536.00	-1.51	221.00	1031.00	-0.37	30.20	220.00	-0.15	16.50	83.44
LT50800142008185GLC00	802	2008-07-03	80	14	162.57	46.45	L1T	5	TM	1.0167	-1.52	193.00	1983.00	-2.84	365.00	1796.00	-1.17	264.00	1536.00	-1.51	221.00	1031.00	-0.37	30.20	220.00	-0.15	16.50	83.44
LT50800152008185GLC00	802	2008-07-03	80	15	160.61	47.59	L1T	5	TM	1.0167	-1.52	193.00	1983.00	-2.84	365.00	1796.00	-1.17	264.00	1536.00	-1.51	221.00	1031.00	-0.37	30.20	220.00	-0.15	16.50	83.44

The Department of the Interior protects and manages the nation's natural resources and cultural heritage; provides scientific and other information about those resources; and honors its special responsibilities to American Indians, Alaska Natives, and affiliated Island Communities.

NPS 953/105935, December 2010

National Park Service
U.S. Department of the Interior

Natural Resource Program Center
1201 Oak Ridge Drive, Suite 150
Fort Collins, Colorado 80525

www.nature.nps.gov